Effects of Brick Pattern on the Static Behavior of Masonry Vaults

Effects of Brick Pattern on the Static Behavior of Masonry Vaults

Claudio Boni[1,a], Daniele Ferretti[1,b*], Erica Lenticchia[2,3c]

[1] *Department of Engineering and Architecture, Università degli Studi di Parma, Parco Area delle Scienze 181/A, 43124 Parma, Italy*

[2] *Department of Structural, Geotechnical and Building Engineering, Politecnico di Torino, Corso Duca degli Abruzzi 24, 10129 Torino, Italy*

[3]*Responsible, Risk, Resilience Interdepartmental Centre (R3C), Politecnico di Torino, Corso Duca degli Abruzzi 24, 10129 Torino, Italy.*

[a] claudio.boni@unipr.it

[b] daniele.ferretti@unipr.it

[c] erica.lenticchia@polito.it

[*] corresponding author

Keywords: masonry vaults, discrete element method, brick texture, static behavior, orthotropic, non-smooth contact dynamics

Abstract

The design of brick masonry vaults has frequently been one of the main topics of historical construction handbooks, where also the orientation of the blocks was an examined issue. However, the influence of brick-texture has not yet been thoroughly investigated computationally. In the present paper the static behavior of masonry vaults of different shapes (barrel, pavilion, and cross vaults), was studied by analyzing and integrating two points of view: one historical and the other computational. First, the instructions provided by ancient documents were described. Then, a Non-Smooth Contact Dynamics Software was used to model vaults with different brick patterns suggested in the past. The vaults were studied with self-weight to observe load descent. Then, a concentrated force was added up to collapse. The analyses show how the load descent and load-bearing capacity are influenced by the brick pattern. Finally, the results of the various analyses were compared with the insights of the past.

1. Introduction

Arches and vaults are archetypal elements of masonry structures that in the course of construction history have assumed different shapes and sizes. The choice of the shape of these structural elements was often due to the need to cover spaces characterized by more or less complex spatiality, by architectural or symbolic needs, or by the loads they had to bear. For a given geometry of the vault, also the masonry texture (or brick pattern) could change according to specific rules. The present work aims to investigate the effect of masonry texture on load descent and load-bearing capacity of masonry vaults. This aspect could permit researchers to better understand the behavior of the vaults and the underlying structures, in order to propose suitable methods for their assessment and strengthening. The choice of the best brick pattern for vaults described in historical treaties and manuals is based on empirical observations of the vault behavior. However, today the problem deserves to be studied also from a structural point of view, using modern numerical methods. The literature on analysis methods for vaults is very extensive and comprises: (a) Trust Network Methods; (b) Finite Element Methods (incremental nonlinear analysis, and limit analysis); (c) Discrete Element Methods. For a comprehensive review, the reader may refer for instance to (Boothby, 2001), (Tralli, et al., 2014) (Marmo & Rosati, 2017). Most numerical studies in the literature focus on the load-bearing capacity of masonry vault without specifically addressing the effect of masonry texture (Tralli, et al., 2014) (D'Altri, et al., 2020). Brick texture generates an orthotropic behavior of the masonry that has been represented for instance by means of plasticity and homogenization models (e.g. (Lourénço, et al., 1997) (Milani, et al., 2006)). In particular, the homogenization technique was used to consider running bond in masonry vaults and domes (Milani, et al., 2008), and herringbone bond in domes (Milani & Cecchi, 2013). Using Discrete Element Method (DEM), (Beatini, et al., 2018) shown that the behavior of domes is influenced by the tensile strength of masonry that arises from its texture. This equivalent tensile strength, also called crosswise tensile strength, results from the contact forces generated by the friction between the blocks and therefore depends on the texture and geometry of the blocks, as well as the compression forces present. Using simple static equations, (Chen & Bagi, 2020) have determined

the value of this crosswise tensile resistance in cases of running bond and herringbone patterns. In addition, the Authors have validated their results by studying cylindrical shells by means of DEM.

The masonry texture has an effect not only on the structural behavior of domes but also on vaults. Recently, (Foti, et al., 2018) analyzed cross vaults subjected to settlements of the supports by means of DEM, confirming that their behavior depends on masonry texture. Forgács, et al. (2018) used DEM to observe the effect of masonry texture in skew arches similar to barrel vaults, while Alforno, et al. (2019) employed micro finite element modelling to study the influence of the brick texture in barrel and cross vaults subjected to displacements of the supports. Apart from a few studies, in the case of vaults, there is a general lack of research on the subject.

The present work wants to address the problem by analyzing three types of vaults: barrel, cross, and pavilion. The work has two souls: one historical and the other computational. Considering the structure of the article, the paper starts with an overview of the brick pattern of masonry vaults used in the past, especially by looking at the historical treatises on architecture and construction. After the identification of the most common brick patterns employed in different vault configurations, the paper continues by illustrating the modeling of vaults by means of DEM. In particular, ProjectChrono, a DEM library developed at the University of Parma, was adopted (ProjectChrono, 2018). The main parameters of the model were calibrated. Then, the model was used to study the static behavior of barrel, cross, and pavilion vaults subjected to self-weight, investigating the load descent. Subsequently, a load was added to the vaults up to failure to observe the effect of the brick pattern on failure load and failure mode. Finally, the results of the various analyses were compared with the insights of the past.

2. Brick patterns of masonry vaults through history

The mechanical behavior of vaults has puzzled architects and scientists for centuries (Benvenuto, 2012) (Huerta Fernández, 2001) (Gaetani, et al., 2016). The works of Benvenuto (Benvenuto, 1981) (Benvenuto, 2012), Como (Como, 2013), Di Pasquale (Di Pasquale, 2001), Heyman (Heyman, 1995),

and Huerta (Huerta Fernández, 2001) (Huerta Fernández, 2008), among others, give an extensive review on the development of the structural analysis and the design of masonry vaults and arches through history. A static theory on arches (and consequently on vaults and domes) was never established in quantitative terms until the end of the 17th century (Benvenuto, 1981). Moreover, the scientific theory of structures for the construction of buildings was not applied until the 19th century. Until then, for centuries, the stability of structures entrusted to the mutual, and proportional, disposal of the parts to avoid the onset of kinematics.

Almost certainly, ancient masons were aware of the importance of the brick texture, i.e., the mutual position of the bricks, not only to shape the thickness of the vaults and to simplify the construction stages, for instance removing the scaffolding, but also to inhibit the formation of cracks improving the behavior of the structure. Unfortunately, the craft of masons was generally handed down from one generation to another and scant information is present in the first treaties.

In this regard, the arrangement of the bricks in masonry vaults and domes was considered a topic belonging to the sphere of building practice for a long time; in fact, it is important to highlight that it was not considered a main topic covered by the authors of early treatises. Alberti generically indicates that arches and vaults must be made in the same way as walls and does not delve into the specific rules regarding the brick pattern; however, as Mainstone (Mainstone, 1969) points out, in [chapter XIV of book III] (Alberti, 1450), Alberti writes that load-carrying groins or ribs, named '*ossatura'*, could be replaced with bricks 'combed' ('*a pettine*') together, as the fingers of two hands joining together. Another example is given by Scamozzi (Scamozzi, 1615), who wrote that thanks to the herringbone brick pattern, the horizontal thrust of the barrel vault is transferred at the corners.

Nevertheless, despite the scarce written information, the fact that the different configurations of brick patterns play an important role in the capacity of masonry vaults had to be known. Wendland (Wendland, 2007) highlights that the construction principles behind the optimal interlocking of blocks were applied to build domes and vaults without formwork, and was especially used for constructing the half-stone vaults.

Filippo Brunelleschi is an example of how construction practice and static intuition coming from a solid knowledge background could merge to create a new extraordinary structural solution. The dome of the Santa Maria del Fiore Cathedral in Florence (Foraboschi, 2016) was built without any centering or formwork, by adding successive self-supporting rings of bricks characterized by a particular herringbone brickwork shown in Figure *1*a. Evidence of the strong influence of Brunelleschi's opera among his contemporaries, regarding the use of brickworks as a solution for the structural stability of large shells, is represented by an artwork stored in Uffizi's "Gabinetto dei Disegni e Stampe", attributed to Antonio da Sangallo il Giovane. The drawing (Figure *1*b) reports the outline of a herringbone brick pattern, in plan and in section, similar to the Brunelleschi's one, together with an explanatory caption "*Volte tonde di mezzane quali si voltano sanza armadura a Firenze*" (transl. vaults built without any formwork in Florence). However, although the Sangallos and other builders of the period employed this method to build large shells without scaffolding (Pizzigoni, et al., 2018), (Taddei & Taddei, 2012), the technique did not spread, and its application was limited to the Italian regions of Tuscany and Lazio (Docci, 2011).

Figure 1*: Examples of herringbone brick patterns: (a) Survey of the brick texture in the Brunelleschi's dome, taken after the removal of some plaster from the dome intradox (Giorgi & Matracchi, 2008) (b)drawing of a vault built without formwork by Cordini Antonio, also known as Antonio da Sangallo il Giovane, stored at the Uffizi's Gabinetto dei Disegni e Stampe (artwork inventory 900 A).*

Therefore, apart from a few exceptions, represented by the authors who focused on stereotomy, it was only with the treaties and manuals published between the second half of the 18th and the beginning of the 20th century that a rich variety of technical literature about the construction of masonry vaults is published. This is mainly due to the fact that the Enlightenment movement led to a different conception of the dissemination of knowledge compared to the past. The cultural revolution and the positivism, that would characterize the nineteenth-century culture, led to a new type of scientific literature: treaties were replaced with "technical manuals" in the interests of the integration between science, practice, and knowledge, in favor of maximum dissemination of knowledge. In this

context, the *Traité théorique et pratique de l'art de bâtir* authored by Rondelet (Rondelet, 1802), is a milestone of the technical literature. Moreover, scholars of the 19th century began to be especially attentive to the analysis of materials and construction techniques, by studying and analyzing architectures from the past: in France, Choisy (Choisy, 1873), (Choisy, 1883) published various books, while Wendland reports a rich overview of the German literature on the subject (Wendland, 2007), which focused in particular on gothic architecture and its solutions for vaulting systems built in stone or half-stone masonry.

Italy also followed the French and German paths, although authors were more concerned about analyzing vernacular architecture and construction techniques, where vaults and arches were built using solid clay brick masonry. In particular, in these technical manuals, the brick pattern required for the different typologies of vaults was reported with detailed descriptions accompanied by technical drawings. Bricks could be positioned in two different configurations, plane or vertical, depending on the vault typology, its rise, and dimensions. A configuration with plane bricks was mainly used for vaults with small spans, located on the upper floors of the buildings, where lower weights are required (Chevalley, 1924).

Various authors (Breymann, 1849), (Chevalley, 1924), (Donghi, 1906), (Formenti, 1893), (Gelati, 1907), (Levi, 1932) report the most common pattern configurations for different vaults typology, and explain when and why it is more preferable to choose a pattern instead of another.

For barrel vaults, various examples of laying are given in the manuals: the simplest method consisted of using the longitudinal row arrangement, i.e. by positioning the courses of bricks parallel to the impost lines (Figure 2a). However, this arrangement is unfavorable for vaults characterized by a large span and a low rise, because the key joints are almost vertical and parallel; consequently, the corresponding courses do not act as wedges and the resistance depends only on the cohesion of the mortar and is therefore limited. In these cases, it was, therefore, preferable to proceed by placing the bricks at 45° degrees with respect to the edges of the plan (Gelati, 1907), (Chevalley, 1924), (Levi,

1932), as shown in Figure 2(b) and (c). However, for Gelati, the optimal solution is represented by Figure 2(d) in which the rows are arched according to the maximum curvature.

Figure 2: Different brick patterns for barrel vaults from an Italian treatise (Gelati, 1907, pp. 214-215): (a) courses parallel to the impost lines; (b) courses at 45° degrees ; (c) courses at 45° degrees with respect to the edges of the plan; (d) courses perpendicular to the impost lines.

Regarding the configuration in Figure 2c, Breymann (1849) adds that another advantage of the pattern is that the pressure of the vault is distributed more on the perimeter walls, where also the front-walls partly act as piers (Breymann, 1849). Gelati also reports a specific pattern for the particular case of an oblique cylindrical vault, which is typically used for staircases (Figure 3a). In this case, it is not advisable to arrange the joints according to the direction of the generating lines, nor according to the directrix, because this would produce oblique thrusts to the wall that would not be counteracted; instead, it is necessary to ensure that the transverse joints are normal to the front planes. Breymann (Breymann, 1849), Formenti (Formenti, 1893), and Chevalley (Chevalley, 1924) report an additional pattern for barrel vaults that differs from the others described previously because the courses start from the middle and close at the piers (Figure *3*b). This solution has the same advantages as the herringbone arrangement, but it allows a more regular finish and consequently does not need plastering (Breymann, 1849).

Figure 3: (a) brick pattern for oblique cylindrical vault (Gelati, 1907, p. 222); (b) additional brick pattern for barrel vault with a more regular finish (Breymann, 1849, p. 39).

The brick patterns of pavilion vaults are similar to the ones of the barrel vaults. Contrary to barrel vaults, the distribution of horizontal thrusts is continuous along the entire perimeter of the supporting walls; therefore, they are not the optimal solution in case there is a need to create several openings. Chevalley highlights how, usually, in pavilion vaults, the bricks are arranged neatly in rows parallel to the impost lines, trying to avoid continuous joints along the edges, which are the weak point of the structure (Chevalley, 1924). However, Guerra (1945) points out that for the pavilion vaults there can be different types of brick-pattern, depending on where one wishes to concentrate the load. In fact, it

is possible to have a texture that tends to concentrate the load in the corners of the walls or to distribute it over their length, depending on the construction criterion of the vertical supports (Guerra, 1945). Donghi reports that many builders use the arrangement showed in Figure 4c, where the rows of bricks are normal to the diagonals. This system has greater strength, as it makes it less easy to disjoin the edges because, in this configuration, the bricks are well concatenated, and the rows form a series of acute arches (Donghi, 1906). When the brick pattern in each quarter of the vault presents normal rows at the diagonals (Figure 4c), it allows the load to be concentrated on the corners; on the contrary, when the rows are parallel to the walls, these tend to be the ones loaded (Figure 4a). In the first case, (Chevalley, 1924) advises reinforcing the edges by thickening them at the extrados.

Figure 4: Brick pattern of pavilion vaults on a rectangular plan (Chevalley, 1924, drawing no XCI, p. 231): (a) courses parallel to the impost lines; (b) mixed configuration, where courses are parallel to the perimeter walls towards the impost and normal to the diagonals in the central part; (c) courses normal to the diagonals; (d) inclined courses.

Finally, there is a mixed configuration, in which the rows are parallel to the perimeter walls towards the impost and normal to the diagonals in the central part (Figure 4b). The herringbone brick pattern instead, was not used very often due to construction complications and the need to cut the corner bricks.

In masonry cross vaults, thrusts are instead concentrated at the corner piers, which represents a great advantage from an architectural point of view since this makes it possible to remove walls and have greater freedom in the distribution of space. Following this design principle, we may find different pattern solutions for cross vaults. For instance, the courses of bricks were arranged in each quarter, normal to the respective arch of impost (Figure 5a), or parallel to them (Figure 5b). Another configuration consisted in rows perpendicular to the diagonal groins (Figure 5c); although this arrangement required greater technical skills of the builders since the rows, joining at the center of each portion, had to be shaped to allow a proper connection. In all these configurations, the aim was to direct the thrust to the corners.

Figure 5: Brick pattern for masonry cross vault where the rows are: (a) normal to the arches (Formenti, 1893, p. 166); (b) parallel to the arches (Guerra, 1945, p. 310); (c) perpendicular to the diagonal groins (Guerra, 1945, p. 309).

Breymann, instead, distinguishes between ribbed cross vaults from the ones made entirely of bricks. Concerning the former case, Breymann writes that masonry ribbed cross vault are usually constructed with a herringbone pattern so that the courses of two adjacent quarters are located in a plane, and the pressure of the vault, which acts according to the edges, is normally transmitted to the groins (Breymann, 1849). With this arrangement, it is also possible to reinforce the connection of the groins with the edges. In the present paper, the ribbed masonry vaults, although they represent an extensive typology set widely spread since the middle ages, will not be analyzed because their behavior is complex and deserves a separate study.

3. Proposed model

In the present work, the static analysis of the vaults was performed using Discrete Element Method (DEM) because it is particularly suitable to model the bricks and the interaction between them. The DEM method was already used in the literature for the analysis of vaults: several studies were performed by means of the commercial software 3DEC (Lemos, 2007), (McInerney & DeJong, 2014), (Lengyel, 2017), (Forgács, et al., 2018), (Foti, et al., 2018). Usually, in DEM the motion equations of the blocks are solved in time by explicit integration algorithms that, requiring small time-steps, are computationally demanding. This aspect limits the maximum number of blocks that can be used. To avoid the problem, a particular type of DEM called Non-Smooth Contact Dynamics (NSCD) was proposed by Moreau and Jean (Moreau, 1988), (Jean, 1999). In NSCD, the interaction between blocks is ruled by Signorini contact condition and Coulomb dry friction law. Implicit integration of the motion equations, written as a function of velocities and impulses, permits to increase the time-step reducing the computational time. NSCD was implemented in the software LMGC90 that was used to study churches (Lancioni, et al., 2013), masonry arches (Chetouane, et al., 2005), (Rafiee & Vinches, 2013), and domes (Rafiee & Vinches, 2016). Independent implementation of NSCD was proposed in

the ProjectChrono open source library (ProjectChrono, 2018). The library was applied to study masonry arches (Beatini, et al., 2019) and domes (Beatini, et al., 2018). The seismic behavior of local mechanisms in a castle was analyzed in (Coïsson, et al., 2016) while (Ferretti, et al., 2017) used the library to study masonry barrel vaults subjected to earthquakes, considering both the presence of linear elastic iron ties and filling, which was modeled with spheres. ProjectChrono was used in (Sicurella, 2017) to study the static behavior of masonry vaults with different brick textures focusing mainly on the modeling phase by means of a 3D CAD parametric tool. Masonry vaults with different brick patterns were analyzed in (Boni, 2018) and (Boni, et al., 2019) considering settlements of the supports. These studies showed the capabilities of ProjectChrono, which was therefore chosen for the present research. ProjectChrono is a C++ open-source middleware that targets the simulation of rigid and flexible body systems with a large number of contacts. A full description of algorithms and equations used in the software is published in (Beatini, et al., 2017). This work is limited to the use of ProjectChrono and therefore a short description is provided, indicating instead the algorithms adopted, among the many available, to allow the reader to repeat the proposed analyses. To this end, the library endorses a formulation based on non-smooth dynamics. Following a Lebesgue decomposition of reactions in continuous and atomic parts, speeds of the bodies can have discontinuous jumps as a function of *bounded variations* (or BV functions), whereas the position of the bodies is described by *absolutely continuous functions* (Beatini, et al., 2017). Contact forces between bodies are handled as *set-valued functions*, and this leads to a time integration algorithm where, at each time step, a cone-complementarity problem is solved (Heyn, et al., 2013) (Mangoni, et al., 2018). The cone complementarity originates from the definition of Coulomb friction cones, to whom all contact reactions must belong when the contact distance is zero. The same coefficient (ruled by parameter *Friction*) is used for both static and dynamic friction. At the cost of solving such complex complementarity problems, one can efficiently simulate simultaneous perfectly rigid contacts. This is a major departure from the more conventional approach of DEM, where contacts are represented by smooth penalty

functions; in fact, the latter approach requires small time-steps, whereas the enhanced stability properties of the non-smooth approach here adopted can simulate complex structures even with large time steps (Beatini, et al., 2017).

To solve the cone complementary problem, obtaining the unknown accelerations and reaction forces at a given time step of the simulation, the Brazilian-Borwein algorithm was used in the present work, providing a maximum number of *Iterations*. Another characteristic of the model is the contact-detecting algorithm, which is based on the Gilbert-Johnson-Keerthi approach (Gilbert, et al., 1988). This method operates on convex surfaces and, in order to solve the problem of degenerate cases, e.g., flat faces with infinite contact points, the algorithm is performed several times at each time-step with small rotational perturbations on blocks, in order to obtain a finite number of possible contact points (Beatini, et al., 2017). For this reason, the number and position of contact points may vary between identical blocks or time steps. Similarly to DEM models, at contact points the approach permits to introduce springs and dashpots (controlled by parameters *Compliance* and *Damping*) to simulate the normal interaction between blocks (Negrut, et al., 2012). The introduction of damping is useful to obtain realistic dynamic solutions but also to dampen slight vibrations of the blocks that may arise from small numerical fluctuating errors related to the solver adopted. To detect possible collisions in advance, a fictitious offset is generated outward to the block (governed by parameter *Envelope*). Similarly, an offset with rounded corners is generated inward to the block (governed by the parameter *Margin*"), to deal with interpenetrations between bodies and wiping out initial small geometrical errors (Beatini, et al., 2019). In the present work, integration in time, which permits to study the evolution of the system during a prescribed time interval, is performed using Euler Implicit Linearized providing a suitable "*Time-step*" (Tasora, 2017).

ProjectChrono was developed to study dynamic problems, nevertheless, it can be used also to analyze steady-state problems providing quasi-static forces and studying the problem for a "*Time-interval*" sufficiently long to allow the system to reach negligible values of kinetic energy. The library of bodies

made available to ProjectChrono is well stocked; in the present work, the bricks were modeled using "convex hull" rigid solids.

4. Calibration of the model and sensitivity analysis of the parameters

4.1 Definition of the model parameters

The ProjectChrono library has been developed in the field of mechanical engineering and to be applied to masonry structures has required a careful calibration of the various parameters, which is described in (Sicurella, 2017) and (Boni, 2018). These parameters can be divided into three categories: (a) interaction between the blocks, ruled by *Compliance*, *Damping* and *Friction*; (b) contact detection, controlled by *Margin* and *Envelope*; (c) solution of the equations in time, governed by *Time-step* and *Time-interval*. The adopted values of these parameters are reported in Table 1.

It is well known that one of the mechanical parameters that govern the real deformation of the vault is the Young modulus of masonry, which also governs its stiffness and thus the load descent. In the proposed model, the deformability of the masonry is not governed by Young's modulus but by the *Compliance* of the springs between the rigid blocks, as well as their texture and size. We used inverse analysis to define the *Compliance* value by simulating a compression test on a masonry wallette.

The wallette had a rectangular cross-section of size 10 cm × 90 cm and a height of 120 cm. It was modeled using rigid blocks of size 10×15×30 cm, reproducing bricks laid horizontally (running bond pattern). Approximately 30 bricks were used to have a representative number of contact points between bricks so that globally the mean behavior of mortar joints is well reproduced. Two additional blocks were inserted at the base and at the top of the wall to simulate the platens of the testing machine. The shortening of the wallette subjected to compression allows calculating an equivalent Young modulus that must coincide with the Young modulus of the masonry measured experimentally or, in our case, to the value for masonry in solid-clay bricks and lime mortar reported in the Italian standard (E = 1500 N/mm^2) (Ministero delle infrastrutture e dei trasporti, 2018). This permitted to

calibrate the value of *Compliance* reported in Table 1. After calibrating *Compliance*, the analysis of the wallette was repeated with herringbone brick texture and vertical brick texture. The configuration with horizontal bricks returns deformability of the wallette that is equivalent to a Young modulus of about 1500 MPa, while the configuration with herringbone bricks corresponds to a Young modulus of about 2000 MPa. This difference is consistent with the fact that in the latter case there are fewer horizontal joints. The configuration with vertical bricks is even stiffer for the same reason, returning a Young modulus of about 2700 MPa, almost twice the value for horizontal bricks, as the number of mortar joints is halved.

For the friction coefficient (*Friction*), the same value discussed in (Beatini, et al., 2019) and (D'Altri, et al., 2020) was chosen. ProjectChrono permits to consider a tensile strength (cohesion) between the blocks; however, it was preferred to neglect it. In historical vaults built with solid-clay bricks and lime mortar, it is often assumed that the small cohesion provided by mortar has lost its effectiveness over time. This hypothesis has also been made recently by (Beatini, et al., 2018) and (Chen & Bagi, 2020) to study by means of DEM the effect of masonry weaving on the apparent tensile strength of masonry.

The default value of the *Damping* coefficient was adopted. Parameters *Margin* and *Envelope* were chosen as a fraction of the smallest dimension of the brick (Sicurella, 2017) (Boni, 2018).

4.2 Validation of the model and sensitivity analysis

After defining the main parameters (Table 1), the model was validated by studying the barrel vault shown in Figure 6 a. The vault was modelled with blocks of dimensions approximately 7×15×30 cm placed in brick rows parallel to the supports. For the boundary conditions, a trapezoidal block fixed at the base was inserted at the two supports (Figure 7a). The vault was loaded with the own weight (with masonry density 1800 kg/m^3 and gravity equal to 9.81 m/s^2) applied immediately at the beginning of the analysis. After a time of 0.2 s, a linear load was added at the keystone (Figure 7a). The load was increased up to failure with a constant rate $\dot{p}$ = 600 Nm^{-1}s^{-1} . The equations of motion were solved with a time-step dt = 10^{-3} s. The solution in time is represented in Figure *8*a, in which y is the

position of the keystone at time t, and y_0 is its initial position. Since the load increases linearly in time, the second axis of the graph shows the corresponding value of the load p. The dimensionless position y/y_0 of the block remains virtually constant over time until the curve begins to fall abruptly, revealing the fall of the block and thus the collapse of the vault. Defining the instant of collapse is not an easy task. Following the work of (Beatini, et al., 2019) on arches, the instant of collapse, called "setting time", can be defined when the displacement of the block reaches a conventional value called "threshold displacement". In our case, this corresponds to a displacement of 0.5 cm and, therefore, to a dimensionless ratio $y/y0 = 0.99$. Analyses were repeated with time-steps equal to 0.8, 1, 1.5, 5 ms. It can be observed that the corresponding curves, represented in Figure *8*a, tend to get closer as the time-step decreases and that the values of "setting time" and collapse load stabilizes. The value $dt = 1$ ms can, therefore, be considered a good compromise between the precision of the results and the computing time.

To understand if the collapse load was influenced by inertial effects, the analysis was repeated for three values of load speed $\dot{p} = 60, 150, 600$ $Nm^{-1}s^{-1}$. The results are represented in Figure *8*b. The curves tend to converge as the load speed decreases, reaching quasi-static conditions. The same figure shows with a dot the failure load computed by modelling the vault as an arch, which is studied with Heyman's method. It can be observed that for slower load speeds $\dot{p}$, the failure load predicted numerically tends to Heyman's theoretical value. *Figure 9*a shows the arch in the undeformed configuration, with the line of thrust obtained with Heyman's method and the corresponding plastic hinges. *Figure 9*b represents a section of the proposed model in the deformed configuration at "setting-time": The two figures present the same position of the plastic hinges. The results of the model in terms of failure load do not coincide perfectly with those of the limit analysis for a number of reasons (including time step, equilibrium in the distorted configuration, etc.) whose detailed examination can be found in Beatini et al. (2019). For our purposes, however, we are not interested in the exact value of the failure load but in its reasonable estimate in order to allow comparisons, even qualitative, between the different cases analyzed.

Table 1 - Values of the parameters of the NSCD model adopted after calibration.

The obtained parameters are valid for vaults made of bricks with dimensions similar to the one used for calibration. These parameters have been adopted for the forthcoming analyses, considering vaults not too different in terms of geometry and modeling every single brick, as done during the calibration process.

5. Static analyses of vaults subjected to self-weight

The quasi-static analyses were performed to highlight how the brick pattern influences the flow, or percolation, of contact forces throughout the vaults subjected to self-weight only. This allows seeing which areas of the vault are most stressed and understanding how the loads are discharged at the supports.

The effect of the brick pattern was studied for three types of vaults: barrel, cross, and pavilion. The geometry of their cross-section is shown in Figure *6*, together with their main dimensions. Barrel vaults have a segmental-arch cross-section (with a central angle of 120° and an internal radius of 1.25 m, Figure 6 a). A round arch with the same radius was used for cross and pavilion vaults (Figure 6 b).

Figure 6 - Geometry of the cross-section of investigated vaults: (a) barrel vaults; (b) cross and pavilion vaults.

The vaults were modeled with "convex hull" rigid blocks (base of about 15×30 cm and thickness of 7 cm or 10 cm) whose number varies from 198 to 373, depending on the type of vault and the brick pattern. The density of masonry was set equal to 1800 kg/m^3, whereas the other parameters of the model are reported in Table 1. In particular, the analyses have been conducted on the whole vault, applying the acceleration of gravity g = 9.81 m/s^2 from the beginning. From a constructive point of view, this is equivalent to the instantaneous removal of the centering (which occurs when removing

with a hammer the folding wedges at the base/top of the props supporting the centering). The gradual removal of the centering (e.g. by emptying the sandbag at the base of the props) could be easily simulated by adding the centering and removing it slowly. Perhaps, in this case, the results may change depending on how and where the centering is removed. During the time, however, the viscosity of the masonry will further change the results. The problem of the construction phases, which is complex, has not been addressed in the present work.

The analysis was carried out waiting for a time of 10 s, which was verified to be sufficient for the dynamic effects to be negligible and the solution to be stable. After this time, the displacements and the contact forces of the blocks were analyzed.

5.1. Barrel vaults

Following the guidelines of ancient treatises, discussed in Section 2, six paradigmatic brick patterns were chosen and investigated: (a) herringbone brick rows to the center (Figure *3* b); (b) herringbone brick rows to edges (Figure *2* c); (c) diagonal brick rows (Figure *2* b); (d) brick rows parallel to supports (Figure *2* a); (e) brick rows perpendicular to supports (Figure *2* d); (f) bricks in a herringbone configuration (Figure *3* a). In the absence of cohesion between blocks, diagonal and herringbone brick rows typologies are not stable. For this reason, walls modelled as rigid blocks fixed at the base were added at the two heads of the vault. The properties of the interface between vault and walls are the same as those adopted for the bricks of the vault. A single block with a trapezoidal cross-section was adopted for each support; the block was fixed to simulate the boundary conditions (Figure *7*a). The number of bricks of the models varies from 314 to 373.

Figure 7: Boundary conditions for: (a) barrel vaults; (b) cross vaults; (c) pavilion vaults.

Figure 8: Sensitivity analysis for a barrel vault. Dimensionless position y/y0 of the keystone of the barrel vault as a function of load p: (a) effect of time-step dt; (b) effect of load rate $\dot{p}$.

Figure 9: Validation of the barrel vault model: (a) Line of thrust and plastic hinges obtained with Heyman's method; (b) Cross-section of the proposed NSCD model where it is possible to observe the position of the hinges.

Results, in terms of force resultant at each contact point between adjacent blocks, are represented in *Figure 10* with red lines whose length is proportional to the force modulus (i.e. the longer the segment, the higher the force). The set of these segments/forces shows the areas of the vault that are more stressed by the flow of forces, allowing to observe where these forces are the higher and which direction they have. Overall, therefore, the representation provides a picture of the flow of forces, also called the percolation of forces.

As can be expected, the layouts with brick rows parallel to supports, perpendicular to supports, and herringbone configuration (*Figure 10* d,e,f) present contact forces that are orthogonal to the axis of the vault. In this case, the behavior of the vaults is similar to the one of many elemental arches placed side by side. The mutual interlocking among these elementary arches, thanks to the toothing between bricks provided by the brick pattern, is different for the three vaults, which may change their response during seismic actions (this topic will be studied in the future).

Differently, for diagonal brick rows (*Figure 10*c), higher contact forces follow the diagonal arches and the reactions at the supports are inclined with respect to the vault axis. Furthermore, smaller contact forces perpendicular to brick rows are present due to friction and lateral compression, which is present because of transverse secondary arches. At the ends of the vault, the arches are shorter and less deformable; therefore, friction occurs between arches of different lengths. Overall, the main behavior of the vault is similar to the one of a diagonal arch. The cases of herringbone brick rows to center and edges (*Figure 10*a,b) are more complex. Contact forces are approximately oriented following the brick rows, but some contact forces are also perpendicular to them; therefore, both transverse and diagonal arches are activated. Furthermore, for herringbone brick rows to center, contact forces are smaller at the edges of the vault. On the contrary, for herringbone brick rows to edges, contact forces show that the vault is also supported by the head walls (not represented in the figure for the sake of clarity), which have a clear static function, confirming the intuition of (Breymann,

1849) and other master builders for this masonry pattern.

Figure 10: Forces flow in barrel vaults under self-weight: (a) Herringbone brick rows to center; (b) Herringbone brick rows to edges; (c) Diagonal brick rows; (d) Brick rows parallel to supports; (e) Brick rows perpendicular to supports; (f) Bricks in a herringbone configuration. Force resultant at each contact point is represented with red lines whose length is proportional to the force magnitude.

Figure 11: Detail of the intersection of the bricks near a groin: (a) Cross vault with rows parallel to the arches; (b) Pavilion vault with rows normal to the impost line.

5.2. Cross vaults

Four types of cross vaults were obtained by intersecting two orthogonal barrel vaults with: (a) brick rows perpendicular to sides (Figure *5* a); (b) brick rows parallel to sides (Figure *5* b); (c) brick rows parallel to diagonals; (d) brick rows perpendicular to diagonals (Figure *5* c). The two latter cases are also referred to as herringbone textures. In the numerical model, the number of bricks varies from 198 to 248. Along the diagonals of the vault, the bricks were toothed, providing interconnection along diagonals (Figure *11*a). Boundary conditions are reproduced by fixing the abutments at their base; in addition, a wall was added at each side of the vault to support brick rows (Figure *7*b). The wall was modeled as a rigid masonry block of size 2.7 × 1.3 × 0.34 m, simply lying on its base to reproduce its actual deformability. Also in this case, gravity was applied immediately, and a picture of the contact forces was taken after 10 s.

For brick rows parallel to sides (Figure 12b), contact forces, which are represented with red segments whose length is proportional to the force magnitude, reveal the formation of arches parallel to the sides. These arches are supported by diagonal arches that transfer the loads to the supports. The diagonal arches are thin and highly stressed, as shown by long contact forces in Figure 12b. In the case of brick rows perpendicular to the sides (Figure 12a), the behavior is similar, but the force-paths are curved, leaving the upper part of the diagonal arches less loaded. For this reason, the stresses are more distributed compared to the previous case. For brick rows parallel to diagonals (Figure 12c), contact

forces flow along the entire vault, still activating wide diagonal arches. The case of brick rows perpendicular to diagonals (Figure 12d) displays a similar behavior, although forces are more concentrated on diagonal arches.

Figure 12: Forces flow in cross vaults under self-weight: (a) Brick rows perpendicular to sides; (b) Brick rows parallel to sides; (c) Brick rows parallel to diagonals; (d) Brick rows perpendicular to diagonals. Force resultant at each contact point is represented with red lines whose length is proportional to the force magnitude.

The analyses confirm that the static behavior of cross vaults is governed by diagonal arches that concentrate the load at the corners, but their characteristics (width and distribution of loads) change with the masonry texture.

5.3. Pavilion vaults

The pavilion vaults that have been analyzed present the same brick patterns adopted for the cross vaults (Figure *13*): (a) brick rows parallel to sides or supports (Figure *4* a); (b) brick rows perpendicular to sides or supports; (c) brick rows parallel to diagonals (Figure *4* c); (d) brick rows perpendicular to diagonals (Figure *4* d). The two latter cases are also referred to as herringbone textures. The number of bricks in the model varies between 224 and 289. Along the diagonals, blocks have been connected, as done for the cross vaults, as shown in Figure *11*b. Bricks at the springers have been fixed (Figure *7*c). Similarly to the previous cases, gravity was applied immediately, and a picture of the contact forces was taken after 10 seconds.

The analyses show that contact forces flow perpendicularly to the supports both for brick rows parallel and perpendicular to them (Figure 13a,b). The vaults behave like many elemental rampant arches of variable length, which depart orthogonally from the supports and reach the diagonals. As pointed out in (D'Ayala & Tomasoni, 2011), the interaction between arches of different lengths (and deformability) generates friction forces that are visible in Figure 13b, where the decomposition in elemental arches is evident. For the case of herringbone textures (Figure 13c,d), contact forces are approximately parallel to brick rows. In particular, for the case of brick rows parallel to diagonals, contact

forces are parallel to both diagonals and the middle of the support is mildly stressed (Figure 13c). Differently, for brick rows perpendicular to diagonals, also the contact forces are perpendicular to both diagonals and converge in the middle of the support, which is more stressed (Figure 13d).

The analyses confirm that also in pavilion vaults subjected to self-weight, the force percolation depends on the brick pattern. Moreover, pavilion vaults behave like many rampant arches, ranging from supports to diagonal arches, whose inclination with respect to the supports depends on the texture of the bricks.

Figure 13: Forces flow in pavilion vaults under self-weight: (a) Brick rows parallel to sides; (b) Brick rows perpendicular to sides; (c) Brick rows parallel to diagonals; (d) Brick rows perpendicular to diagonals. Force resultant at each contact point is represented with red lines whose length is proportional to the force magnitude.

6. Failure analyses of vaults subjected to a concentrated force

Previous analyses have shown that the static behavior of vaults subjected to self-weight depends on the masonry texture. In this paragraph, we analyze the behavior of the same vaults subjected to an additional concentrated load that brings them to collapse to understand if the ultimate load and the mode of failure change with the texture. Rather than using an unevenly distributed load representing the filling, it was preferred to use a concentrated load because it is more easily reproducible. Therefore, the entire model was subject to gravity from the beginning and then the concentrated load was applied after 0.2 s with a constant rate up to failure.

6.1. Barrel vaults

The barrel vaults studied in paragraph 5.1 have been loaded by their self-weight and an additional linear load parallel to the supports and applied along the key. The load was increased with a speed of 600 $Nm^{-1}s^{-1}$ until the vault collapsed. *Figure 14* shows the contact forces for the different cases examined at the beginning of the vaults collapse. Figure 15 represents the position y at time t of a point in the key divided by the initial position (rise of the vault) y_0 as the load p increases. The

abrupt change in the curve identifies the collapse of the vault. The barrel vault with brick rows parallel to supports is the weakest because the hinges of the collapse mechanism develop directly along the alignment of the brick rows (*Figure 14*d). In the other cases, the brick pattern and, to a lesser extent, the sliding and dilatancy between the bricks cause the formation of compressive forces that are discharged on the header walls with activation of transversal arches. This aspect is particularly evident for herringbone brick rows to edges (*Figure 14*b) and diagonal brick rows (*Figure 14*c). By changing the texture, the load-bearing capacity of the vault increases significantly, as can be seen in Figure 15.

The analyses, therefore, confirm the recommendations of 19th-century treaties on the role of header walls: diagonal brick rows or herringbone brick rows to edges are suggested in case of long spans, whereas brick rows parallel to supports are advisable just for short spans.

Figure 14: Forces flow in barrel vaults under line load: (a) Herringbone brick rows to the center; (b) Herringbone brick rows to edges; (c) Diagonal brick rows; (d) Brick rows parallel to supports; (e) Brick rows perpendicular to supports; (f) Bricks in a herringbone configuration. Force resultant at each contact point is represented with red lines whose length is proportional to the force magnitude.

Figure 15: Barrel vaults with different brick patterns: dimensionless position of the key y/y_0 as a function of the applied load p.

6.2. Cross vaults

The cross vaults were analyzed with self-weight applied from the beginning and a concentrated force on the keystone increasing with a speed of 1.5 kN/s. In all cases, the forces descend following the diagonal arches, but crossing with portions of different widths (*Figure 16*). *Figure 17* shows that, also in this case, the value of ultimate load *P* depends on the masonry texture. Brick rows parallel or perpendicular to diagonals provide better performances.

Figure 16: Forces flow in cross vaults under a concentrated force in the key: (a) Brick rows perpendicular to sides; (b) Brick rows parallel to sides; (c) Brick rows parallel to diagonals; (d) Brick rows perpendicular to diagonals. Force resultant at each contact point is represented with red lines whose length is proportional to the force magnitude.

Figure 17: Cross vaults with different brick patterns: dimensionless position of the key y/y_0 as a function of the applied load P.

6.3. Pavilion vaults

The pavilion vaults were analyzed with self-weight applied from the beginning of the analysis and a concentrated force on the keystone after 0.2 s increasing with a speed of 1.5 kN/s. For brick rows parallel to supports and perpendicular to supports, the load goes down following the medians of the square (*Figure 18*a,b). Instead, the diagonal arches are activated in the case of herringbone textures (*Figure 18*c,d). As can be seen in *Figure 19*, also in this case, the load-bearing capacity changes considerably with the brickwork texture, with better strength with brick rows perpendicular or parallel to the diagonals. This result is in disagreement with the indications of (Chevalley, 1924), according to which this texture should be avoided because it generates a discontinuity on the diagonals that tend to open, but it is consistent with what is reported in other manuals (Donghi, 1906) (Guerra, 1945).

Figure 18: Forces flow in pavilion vaults under a concentrated force in the key: (a) Brick rows parallel to sides; (b) Brick rows perpendicular to sides; (c) Brick rows parallel to diagonals; (d) Brick rows perpendicular to diagonals. Force resultant at each contact point is represented with red lines whose length is proportional to the force magnitude.

Figure 19: Pavilion vaults with different brick patterns: Dimensionless position of the key y/y_0 as a function of the applied load P.

7. Conclusions

The purpose of the current study was to determine the effect of masonry texture on the static behavior of vaults. First, the instructions on the masonry texture provided by ancient manuals and treatises were searched. To study the effect of these textures, it was decided to model the individual bricks of the vault using the Non-Smooth Contact Dynamics Software ProjectChrono. The parameters of the software were calibrated and validated by modelling a simple barrel vault. Then, the software was used to model barrel vaults, cross vaults, and pavilions with different masonry textures. Initially, the vaults were studied applying the self-weight alone. Subsequently, a concentrated force was added,

leading the vaults to collapse. The analyses have shown that:

- The descent of the loads in the vaults changes with the masonry texture and, consequently, the distribution of the actions that the vaults exert on the underlying walls changes.
- The collapse load of vaults changes with the brick texture. This can be explained by the different descent of loads but also by the presence of an apparent tensile strength that arises from the interlocking of the bricks (cross-wise tensile strength).
- Often, the vaults are modeled using elementary arches. The choice of these elementary arches should depend on the descent of forces and, for this reason, could be varied with the brick texture.

Moreover, the analyses confirm the suggestions that can be found in some 19th-century manuals. These empirical insights, based essentially on in situ observation of vault behavior, deformations and cracks, are still valid today.

Finally, it is important to highlight how a better understanding of masonry vault construction techniques is not only interesting from a historical point of view, but it is also important for the preservation of the architectural heritage because it leads to a better analysis of its structural behavior and permits to perform more effective restorations choices.

Acknowledgements

The authors thank Prof. Alessandro Tasora for the technical support in using software ProjectChrono.

References

Alberti, L. B., 1450. *De re aedificatoria.* Firenze: ..

Alforno, M., Calderini, C., Monaco, A. & Venuti, F., 2019. *Numerical modelling of masonry vaults with different brick pattern.* Barcelona, International Association for Shell and Spatial Structures (IASS), pp. 1-8.

Beatini, V., Royer Carfagni, G. & Tasora, A., 2017. A regularized non-smooth contact dynamics approach for architectural masonry structures. *Computer & Structures,* Volume 187, pp. 88-100.

Beatini, V., Royer-Carfagni, G. & Tasora, A., 2018. The role of frictional contact of constituent blocks on the stability of masonry domes. *Proceedings of the Royal Society A. Mathematical, Physical and Engineering Sciences,* 474(2209), pp. 1-21.

Beatini, V., Royer-Carfagni, G. & Tasora, A., 2019. Modeling the shear failure of segmental arches. *International Journal of Solids and Structures,* Volume 158, pp. 21-39.

Benvenuto, E., 1981. *La scienza delle costruzioni e il suo sviluppo storico..* Firenze: Sansoni.

Benvenuto, E., 2012. *An introduction to the history of structural mechanics.* New York: Springer Science & Business Media.

Boni, C., 2018. *Analysis of masonry vaults with discrete element method: brick pattern effect,* Italy: MSc Thesis, University of Parma. Supervisors: Prof. Ferretti, D. & Dr. Lenticchia, E..

Boni, C., Ferretti, D., Lenticchia, E. & Tasora, A., 2019. *DEM modelling of masonry vaults: influence of brick pattern and infill on stability during supports displacements.* Barcelona, International Association for Shell and Spatial Structures (IASS).

Boothby, T. E., 2001. Analysis of masonry arches and vaults. *Progress in Structural Engineering and Materials,* 3(3), pp. 246-256.

Breymann, G. A., 1849. *Allgemeine Bau-Constructions-Lehre, mit besonderer Beziehung auf das Hochbauwesen ein Leitfaden zu Vorlesungen und zum Selbstunterrichte.* Stuttgart: Hoffmann.

Chen, S. & Bagi, K., 2020. Crosswise tensile resistance of masonry patterns due to contact friction. *P. Roy. Soc. A-Math Phy,* p. https://doi.org/10.1098/rspa.2020.0439.

Chetouane, B., Dubois, F., Vinches, M. & Bohatier, C., 2005. NSCD discrete element method for modelling masonry structures. *International journal for numerical methods in engineering,* Volume 64, pp. 65-94.

Chevalley, G., 1924. *Elementi di tecnica dell'architettura: materiali da costruzione e grosse strutture.* Torino: Pasta.

Choisy, A., 1873. *L'art de bâtir chez les Romains.* Paris: Ducher et C.ie.

Choisy, A., 1883. *L'Art de bâtir chez les Byzantins.* Paris: Librairie de la Société Anonyme de Publications Periodiques.

Como, M., 2013. *Statics of historic masonry constructions.* Berlin Heidelberg: Springer.

Coïsson, E., Ferrari, L., Ferretti, D. & Rozzi, M., 2016. Non-smooth dynamic analysis of local seismic damage mechanisms of the San Felice Fortress in Northern Italy. *Procedia Engineering,* Volume 161, pp. 451-457.

D'Altri, A. M. et al., 2020. Historic barrel vaults undergoing differential settlements. *Int. J. Archit. Herit.,* 14(8), pp. 1196-1209.

D'Ayala, D. F. & Tomasoni, E., 2011. Three-dimensional analysis of masonry vaults using limit state analysis with finite friction. *International Journal of Architectural Heritage,* Volume 5, pp. 140-171.

Di Pasquale, S., 2001. *L'arte del costruire tra conoscenza e scienza.* Venezia: Marsilio Editore.

Docci, M., 2011. Le volte autoportanti apparecchiate a spina pesce.. In: *Le cupole Murarie: Storia, Analisi, Intervento.* Roma: Edizioni PRE progetti, pp. 383-391.

Donghi, D., 1906. *Manuale dell'Architetto. Compilato sulla traccia del Bakunde des Architekten.* Torino: Utet.

Ferretti, D., Coïsson, E. & Rozzi, M., 2017. A New Numerical Approach to the Structural Analysis of Masonry Vaults. *Key Engineering Materials,* Volume 747, pp. 52-59.

Foraboschi, P., 2016 . The central role played by structural design in enabling the construction of buildings that advanced and revolutionized architecture. *Construction and Building Materials,* Volume 114, pp. 956-976 .

Forgács, T., Sarhosis, V. & Bagi, K., 2018. Influence of construction method on the load bearing capacity of skew masonry arches. *Engineering Structures,* Volume 168, pp. 612-627.

Formenti, C., 1893. *La pratica del fabbricare per l'ingegnere.* Milano: Ulrico Hoepli.

Foti, D., Vacca, V. & Facchini, I., 2018. DEM modeling and experimental analysis of the static behavior of a dry-joints masonry cross vaults. *Construction and Building Materials,* 5, Volume 170, pp. 111-120.

Gaetani, A., Monti, G., Lourenço, P. B. & Marcari, G., 2016. Design and Analysis of Cross Vaults Along History. *International Journal of Architectural Heritage,* 2, Volume 10, pp. 841-856.

Gelati, C., 1907. *Nozioni pratiche ed artistiche di architettura.* 2nd edition (1st edition, 1899) a cura di Torino: Carlo Pasta.

Gilbert, E. G., Johnson, D. W. & Keerthi, S. S., 1988. A fast procedure for computing the distance between complex objects in three-dimensional space. *IEEE Journal on Robotics and Automation,* Volume 4, pp. 193-203.

Giorgi, L. & Matracchi, P., 2008. *New studies on Brunelleschi's dome in Florence.* Bath, UK, Taylor & Francis Group, p. 191–198.

Guerra, C., 1945. *Architettura tecnica - le strutture degli edifici (parte prima).* 3rd edition a cura di Napoli: Casa Editrice Raffaele Pironti.

Heyman, J., 1995. *The stone skeleton: structural engineering of masonry architecture..* Cambridge: Cambridge University Press.

Heyn, T., Anitescu, M., Tasora, A. & Negrut, D., 2013. Using Krylov subspace and spectral methods for solving complementarity problems in many-body contact dynamics simulation. *International Journal for Numerical Methods in Engineering,* 95(7), pp. 541-561.

Huerta Fernández, S., 2001. Mechanics of masonry vaults: The equilibrium approach. In: P. B. Lourenco & P. Roca, a cura di *Historical Constructions. Possibilities of numerical and experimental techniques* . Guimaraes: Universidade do Minho, pp. 47-69.

Huerta Fernández, S., 2008. The analysis of masonry architecture: a historical approach. *Architectural Science Review,* Volume 51, pp. 297-328.

Jean, M., 1999. The non-smooth contact dynamics method. *Comput. Methods Appl. Mech. Eng.,* Volume 177, pp. 235-257.

Lancioni, G., Lenci, S., Piattoni, Q. & Quagliarini, E., 2013. Dynamics and failure mechanisms of ancient masonry churches subjected to seismic actions by using the NSCD method: The case of the medieval church of S. Maria in Portuno. *Engineering Structures,* Volume 56, pp. 1527-1546.

Lemos, J. V., 2007. Discrete element modeling of masonry structures. *International Journal of Architectural Heritage,* Volume 1, pp. 190-213.

Lengyel, G., 2017. Discrete element analysis of gothic masonry vaults for self-weight and horizontal support displacement. *Engineering Structures,* 10, Volume 148, pp. 195-209.

Levi, C., 1932. *Trattato teorico pratico di costruzioni civili, rurali, stradali ed idrauliche.* Milano: Hoepli.

Lourénço, B. P., De Borst, R. & Rots, J. G., 1997. A plane stress softening plasticity model for orthotropic materials. *Int. J. Num. Meth. Eng.,* 40(21), pp. 4033-4057.

Mainstone, R. J., 1969. Brunelleschi's Dome of S. Maria del Fiore and some Related Structures. *Transactions of the Newcomen Society,* 42(1), pp. 107-126.

Mangoni, D., Tasora, A. & Garziera, R., 2018. A primal-dual predictor-corrector interior point method for non-smooth contact dynamics. *Computer Methods in Applied Mechanics and Engineering,* Volume 330, pp. 351-367.

Marmo, F. & Rosati, L., 2017. Reformulation and extension of the thrust network analysis. *Computers and Structures,* Issue 182, pp. 104-118.

McInerney, J. & DeJong, M. J., 2014. Discrete Element Modeling of Groin Vault Displacement Capacity. *International Journal of Architectural Heritage,* 11, Volume 9, pp. 1037-1049.

Milani, E., Milani, G. & Tralli, A. M., 2008. Limit analysis of masonry vaults by means of curved shell finite elements and homogeneization. *Int. J. Solids Struct.,* Volume 45, pp. 5258-5288.

Milani, G. & Cecchi, A., 2013. Compatible model for herringbone bond masonry: Linear elastic homogenization, failure surfaces and structural implementation. *Int. J. of Solids and Struct.,* Volume 50, pp. 3274-3296.

Milani, G., Lourenço, P. B. & Tralli, A. M., 2006. Homogenised limit analysis of masonry walls, Part I: Failure surfaces. *Comp. & Struct.,* 84(3-4), pp. 166-180.

Ministero delle infrastrutture e dei trasporti, 2018. *Italian Code for Structural Design, Norme Tecniche per le Costruzioni, D.M. 17/1/2018, (GU Serie Generale n.42 del 20-02-2018 - Suppl. Ordinario n. 8) (In Italian)..* s.l.:s.n.

Moreau, J. J., 1988. Unilateral contact and dry friction in finite dimension freedom dynamics. *CISM Courses and Lectures, Springer, Berlin,* Volume 302, pp. 1-82.

Negrut, D. et al., 2012. Leveraging parallel computing in multibody dynamics. *Multibody System Dynamics,* Volume 27, p. 95–117.

Pizzigoni, A. et al., 2018. *Herringbone naked structure A visual survey of the dome of Santa Maria in Ciel d'Oro.* MIT, Boston, USA, International Association for Shell and Spatial Structures (IASS).

ProjectChrono, 2018. *ProjectChrono. An Open Source Multi-physics Simulation Engine.* [Online] Available at: https://projectchrono.org

Rafiee, A. & Vinches, M., 2013. Mechanical behaviour of a stone masonry bridge assessed using an implicit discrete element method. *Engineering Structures,* Volume 48, pp. 739-749.

Rafiee, A. & Vinches, M., 2016. Implicit discrete element analysis of a masonry cupola under seismic loads. *International Journal of Civil Engineering,* Volume 14, pp. 357-367.

Rondelet, J. B., 1802. *Traité théorique et pratique de l'art de bâtir.* Paris: F. Didot.

Scamozzi, V., 1615. *L'idea della architettura universale.* Venezia, Italy: s.n.

Sicurella, C., 2017. *The role of masonry pattern in vaultsfrom parametric algoritmic design to staticanalysis by discrete element method,* Italy: MSc Thesis, University of Parma. Supervisors: Prof. Ferretti, D. & Dr. Lenticchia, E..

Taddei, A. & Taddei, D., 2012. *The "spina-pesce" and the "corda- blanda": florentine tradition in the (self-supporting) domes rotating.* Firenze, Nardini Editore.

Tasora, A., 2017. *Time integration in Chrono::Engine.* [Online]
Available at: http://www.projectchrono.org/assets/white_papers/ChronoCore/integrator.pdf

Tralli, A., Alessandri, C. & Milani, G., 2014. Computational Methods for Masonry Vaults: A Review of Recent Results. *The Open Civil Engineering Journal,* 10, Volume 8, pp. 272-287.

Wendland, D., 2007. Traditional vault construction without formwork: Masonry pattern and vault shape in the historical technical literature and in experimental studies. *International Journal of Architectural Heritage,* 1 (4), p. 311–365.

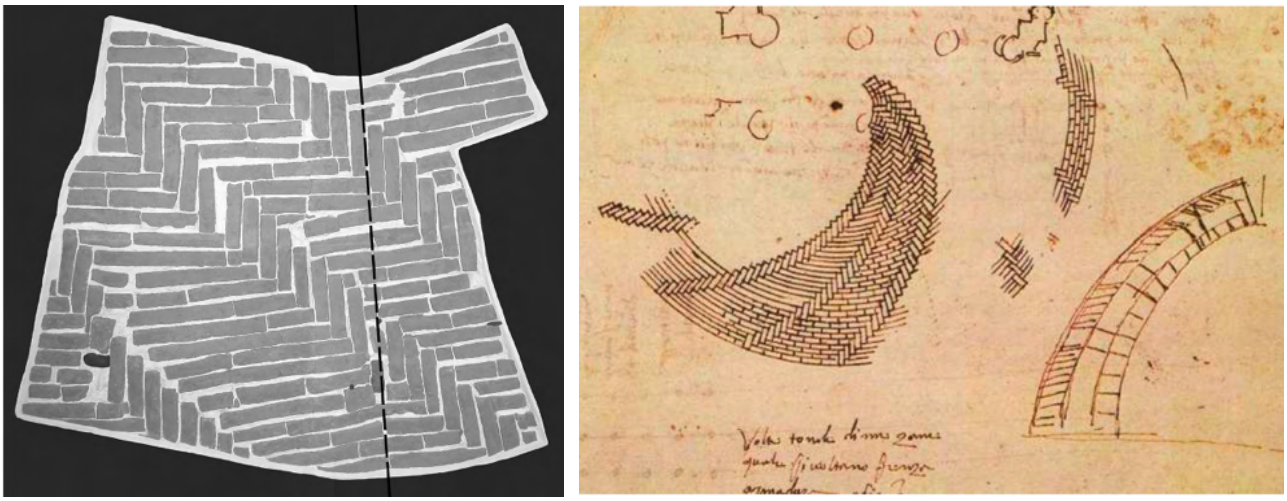

(a) (b)

Figure 1: (a) Examples of herringbone brick patterns: (a) Survey of the brick texture in the Brunelleschi's dome, taken after the removal of some plaster from the dome intradox *(Giorgi & Matracchi, 2008)* (b) drawing of a vault built without formwork by Cordini Antonio, also known as Antonio da Sangallo il Giovane, stored at the Uffizi's Gabinetto dei Disegni e Stampe (artwork inventory 900 A).

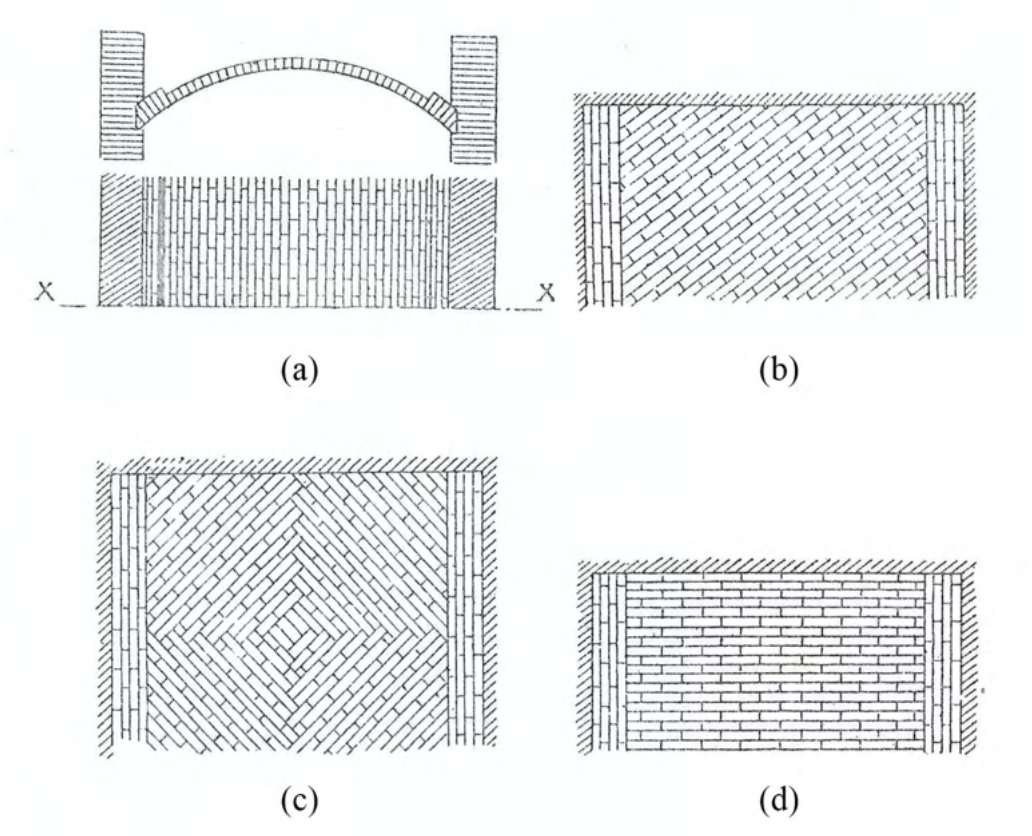

Figure 2: Different brick patterns for barrel vaults from an Italian treatise *(Gelati, 1907, pp. 214-215)*: (a) courses parallel to the impost lines; (b) courses at 45° degrees ; (c) courses at 45° degrees with respect to the edges of the plan; (d) courses perpendicular to the impost lines.

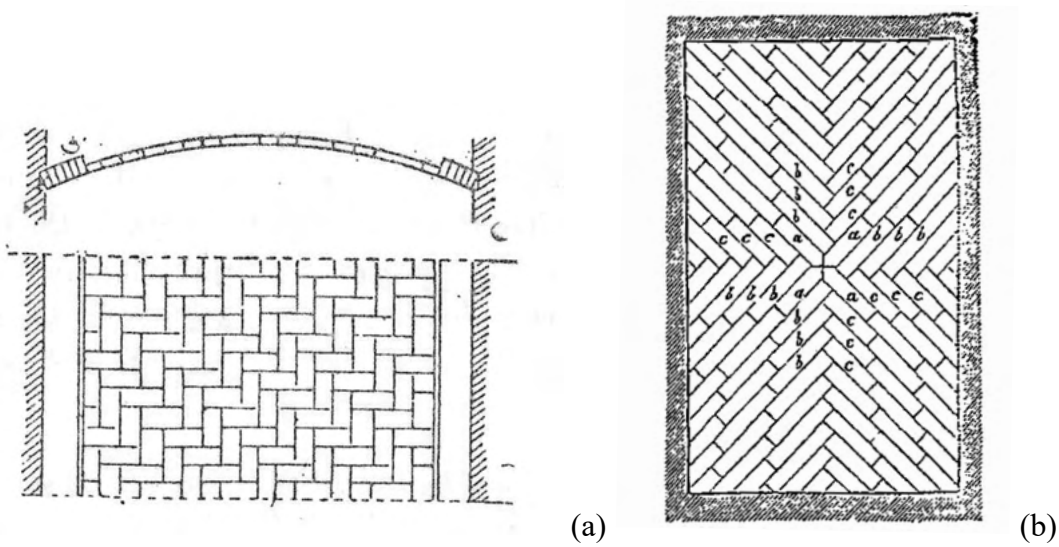

(a) (b)

Figure 3: (a) Brick pattern for oblique cylindrical vault *(Gelati, 1907, p. 222)*; (b) Additional brick pattern for barrel vault with a more regular finish *(Breymann, 1849, p. 39)*.

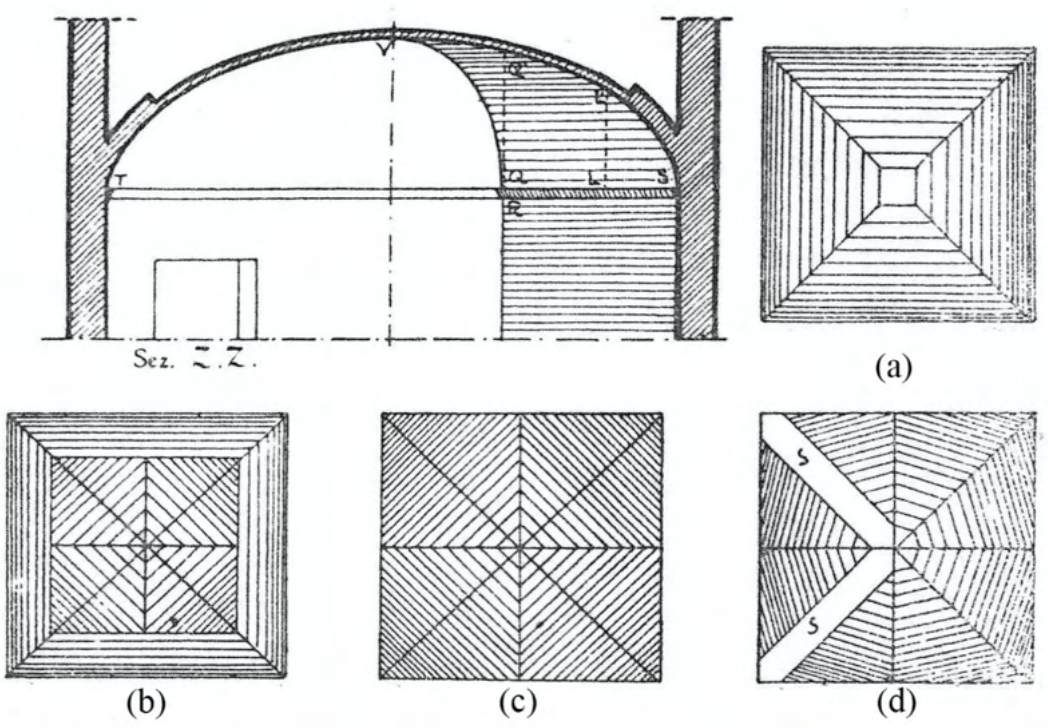

Figure 4: Brick pattern of pavilion vaults on a rectangular plan *(Chevalley, 1924, drawing no XCI, p. 231)*: (a) courses parallel to the impost lines; (b) mixed configuration, where courses are parallel to the perimeter walls towards the impost and normal to the diagonals in the central part; (c) courses normal to the diagonals; (d) inclined courses.

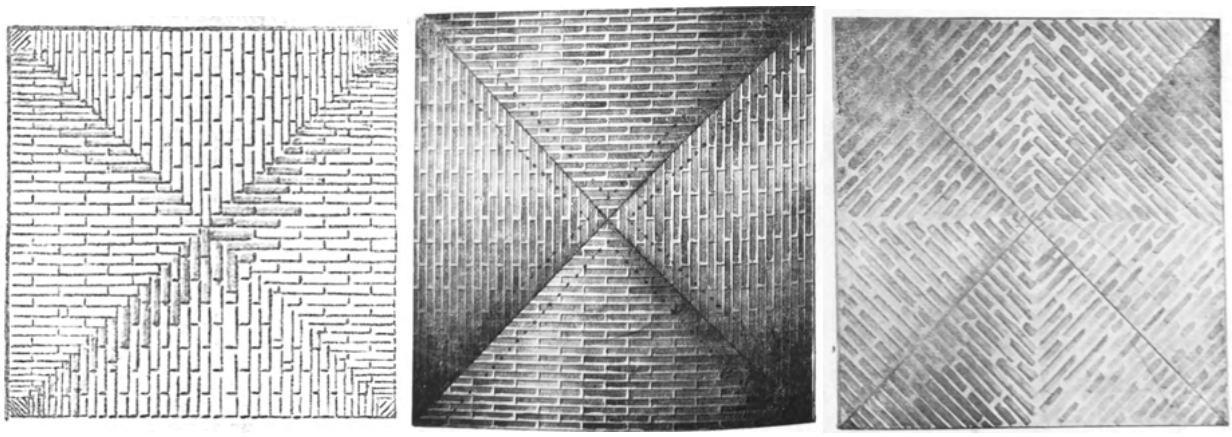

(a) (b) (c)

Figure 5: Brick pattern for masonry cross vault where the rows are: (a) normal to the arches (Formenti, 1893, p. 166); (b) parallel to the arches (Guerra, 1945, p. 310); (c) perpendicular to the diagonal groins (Guerra, 1945, p. 309).

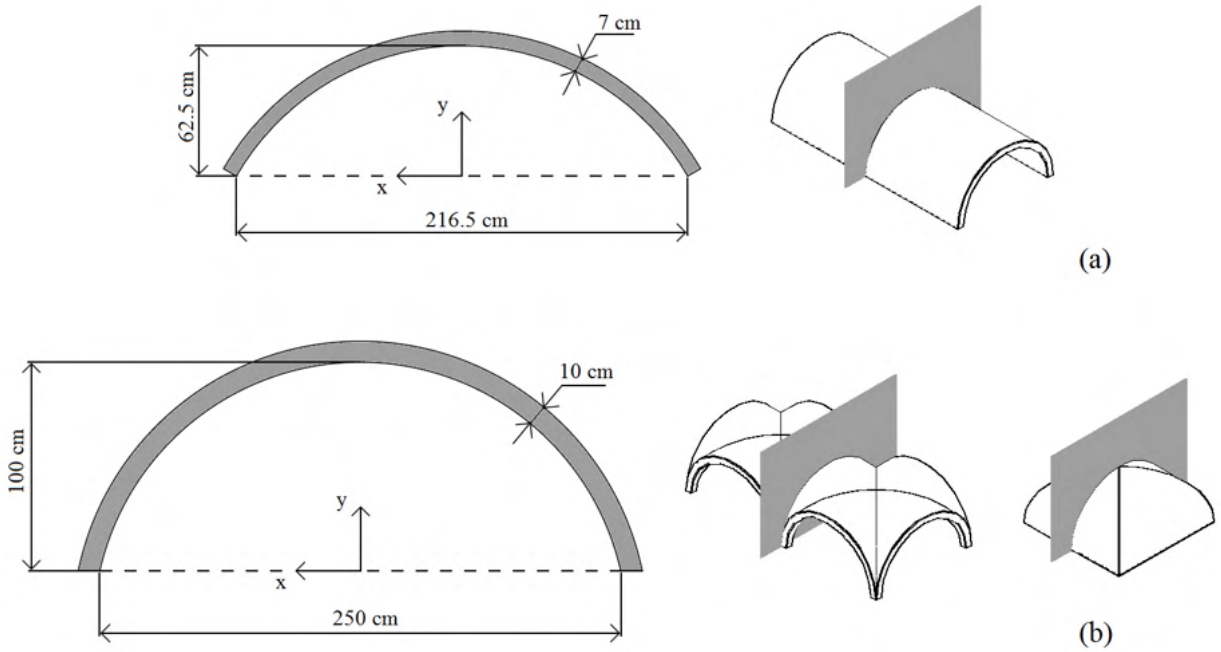

Figure 6: Geometry of the cross-section of the vaults: (a) barrel vaults; (b) cross and pavilion vaults.

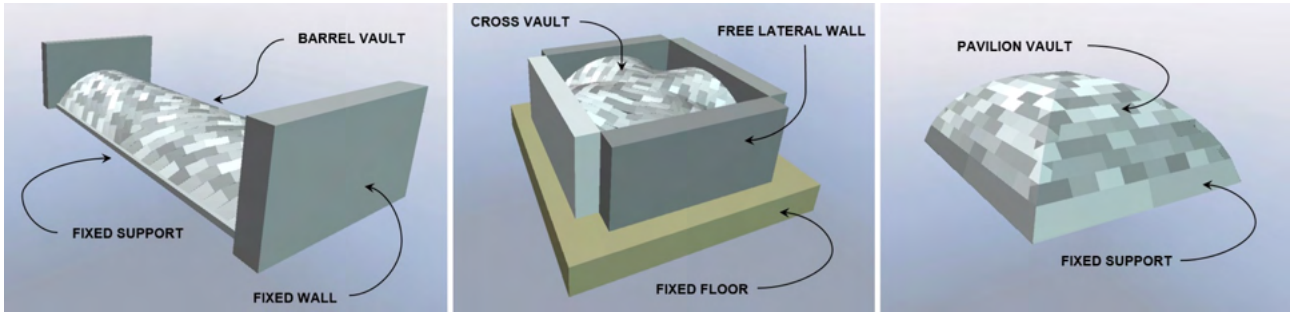

(a) (b) (c)

Figure 7: Boundary conditions for: (a) barrel vaults; (b) cross vaults; (c) pavilion vaults.

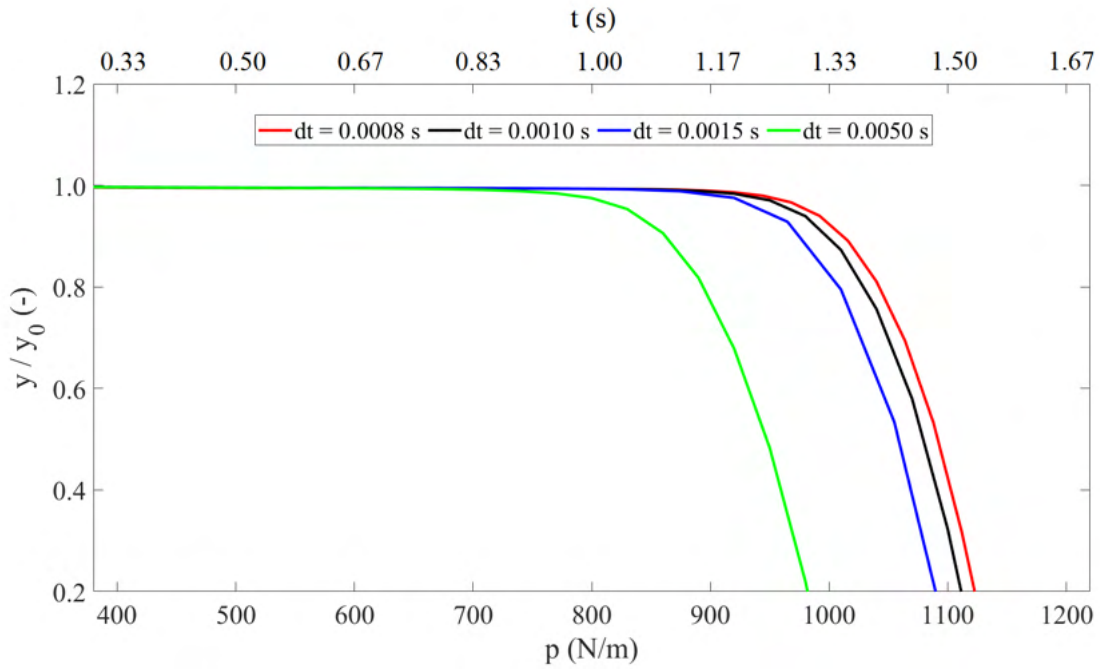

(a)

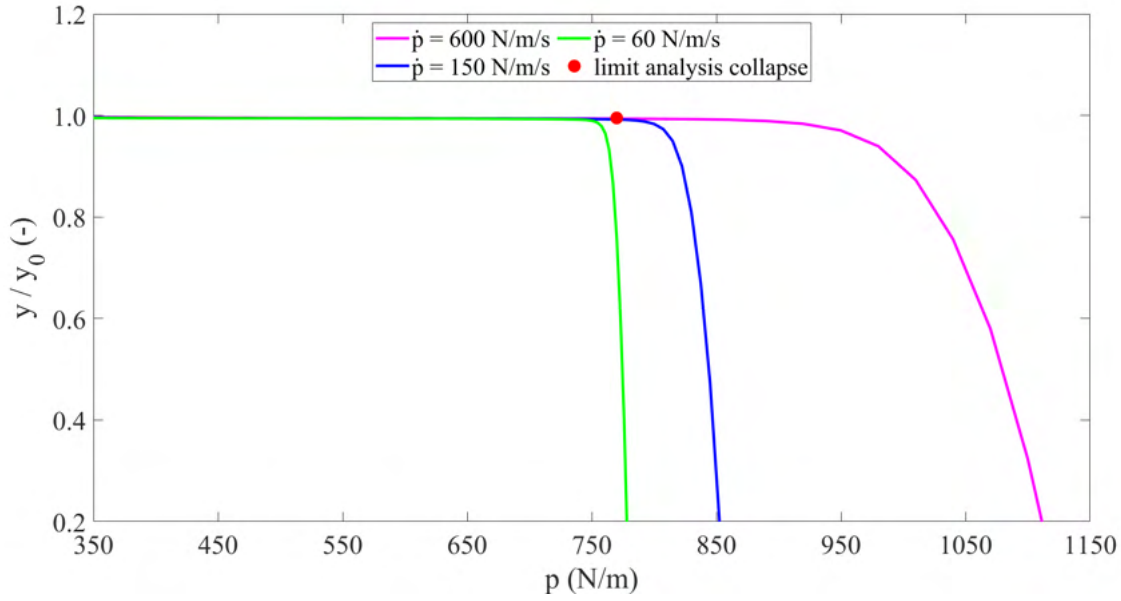

(b)

Figure 8: Sensitivity analysis for a barrel vault. Dimensionless position y/y0 of the keystone of the barrel vault as a function of load p: (a) effect of time-step dt; (b) effect of load rate $\dot{p}$.

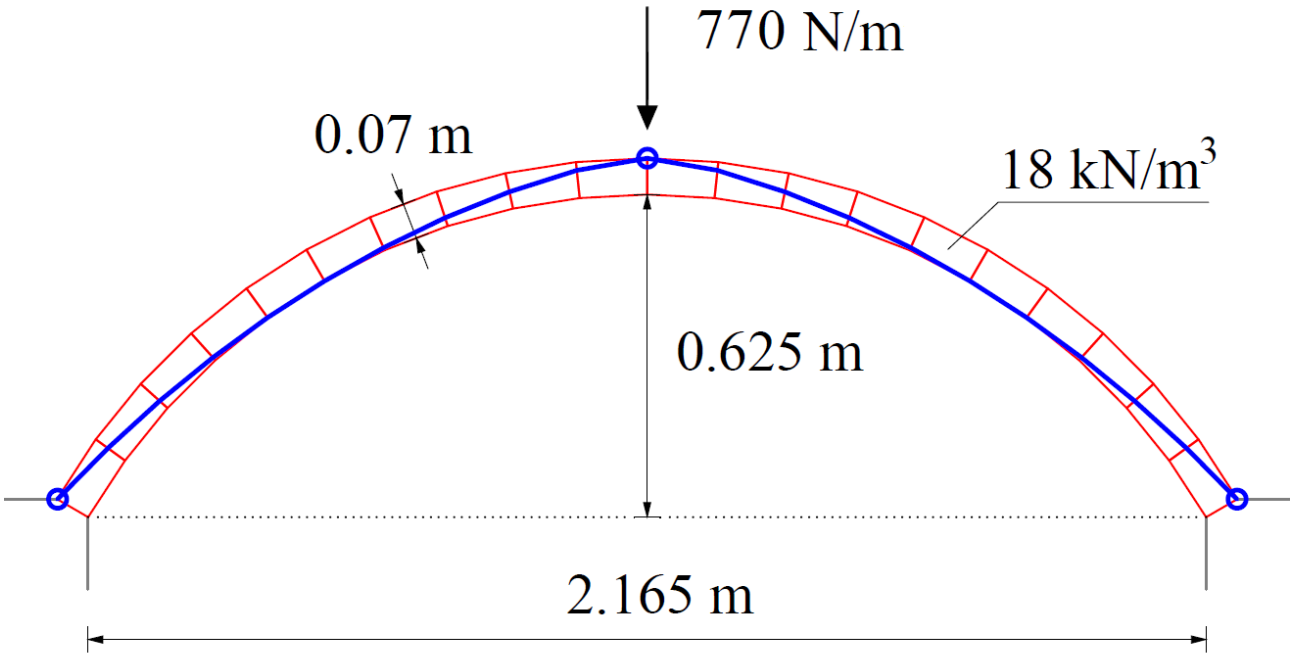

(a)

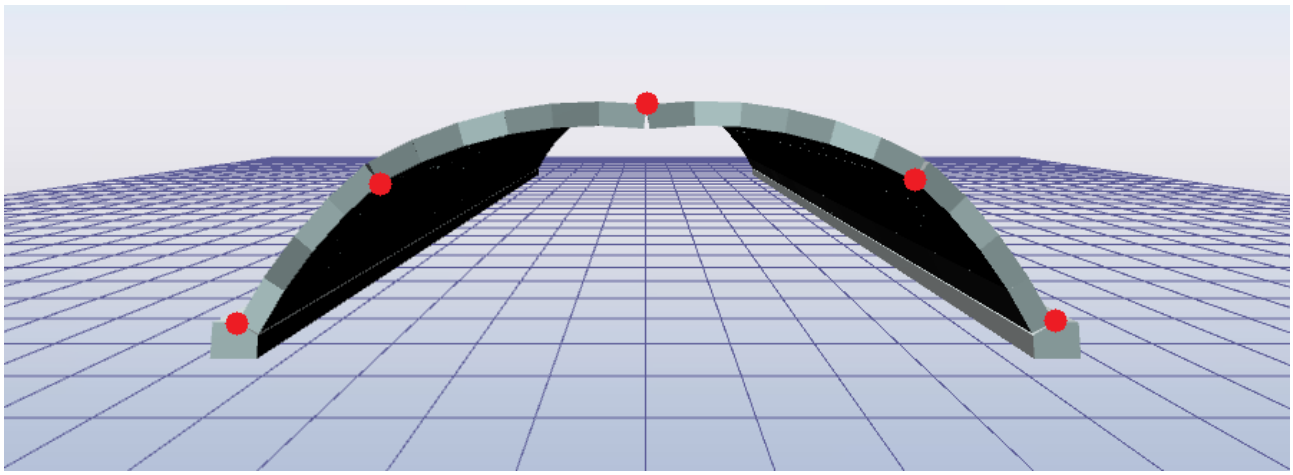

(b)

Figure 9: Validation of the barrel vault model: (a) Line of thrust and plastic hinges obtained with Heyman's method; (b) Cross section of the proposed NSCD model where it is possible to observe the position of the hinges.

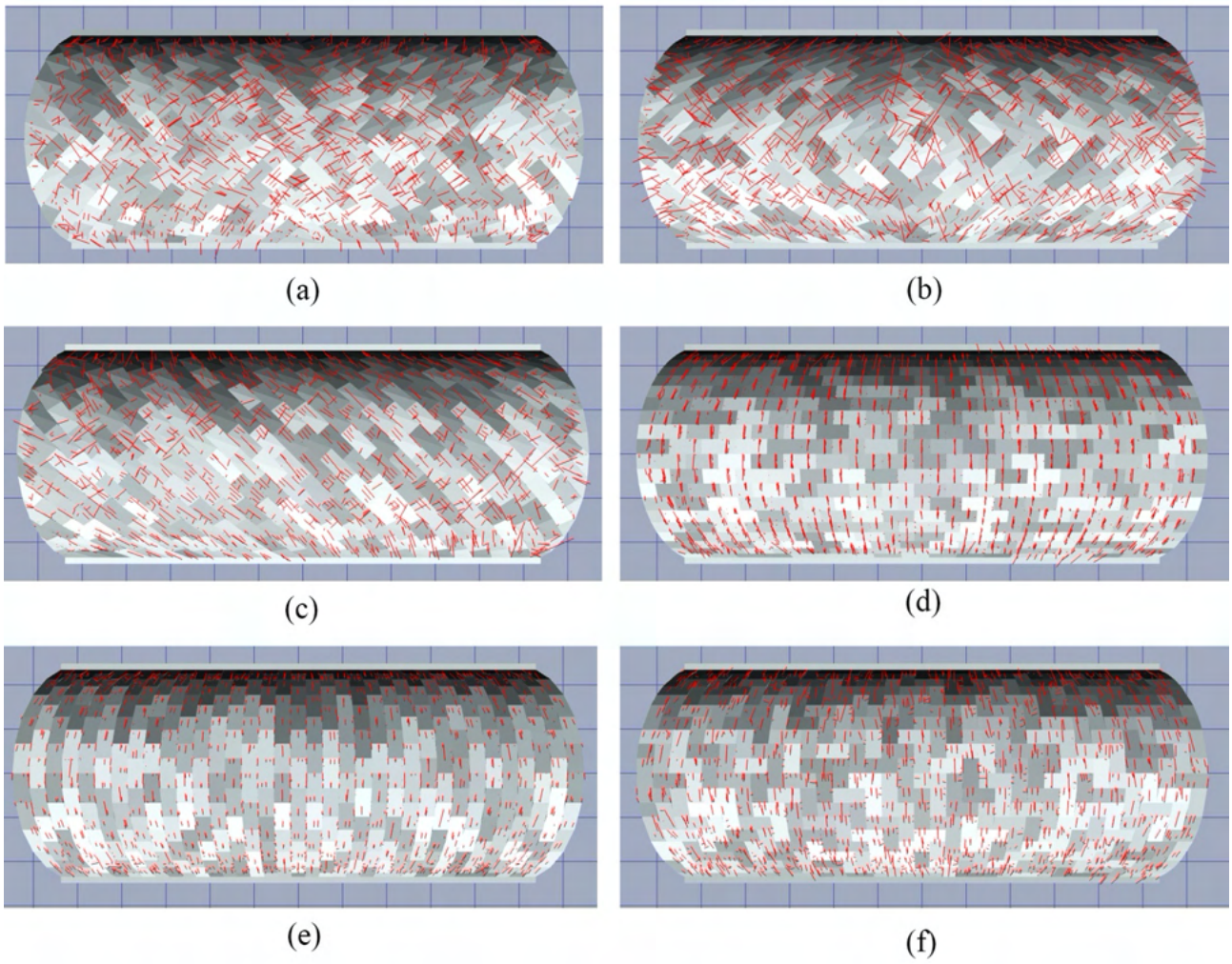

Figure 10: Forces flow in barrel vaults under self-weight: (a) Herringbone brick rows to center; (b) Herringbone brick rows to edges; (c) Diagonal brick rows; (d) Brick rows parallel to supports; (e) Brick rows perpendicular to supports; (f) Bricks in a herringbone configuration. Force resultant at each contact point is represented with red lines whose length is proportional to the force magnitude.

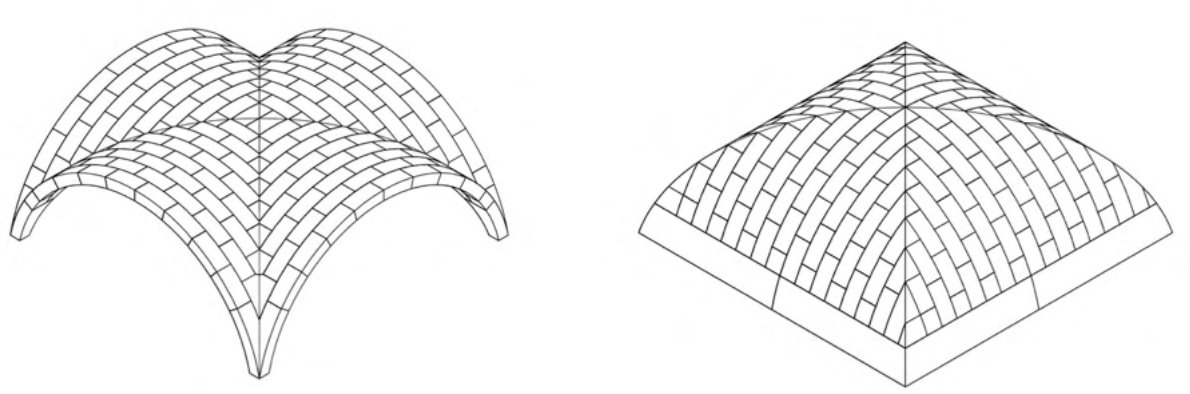

(a) (b)

Figure 11: Detail of the intersection of the bricks near a groin: (a) Cross vault with rows parallel to the arches; (b) Pavilion vault with rows normal to the impost line.

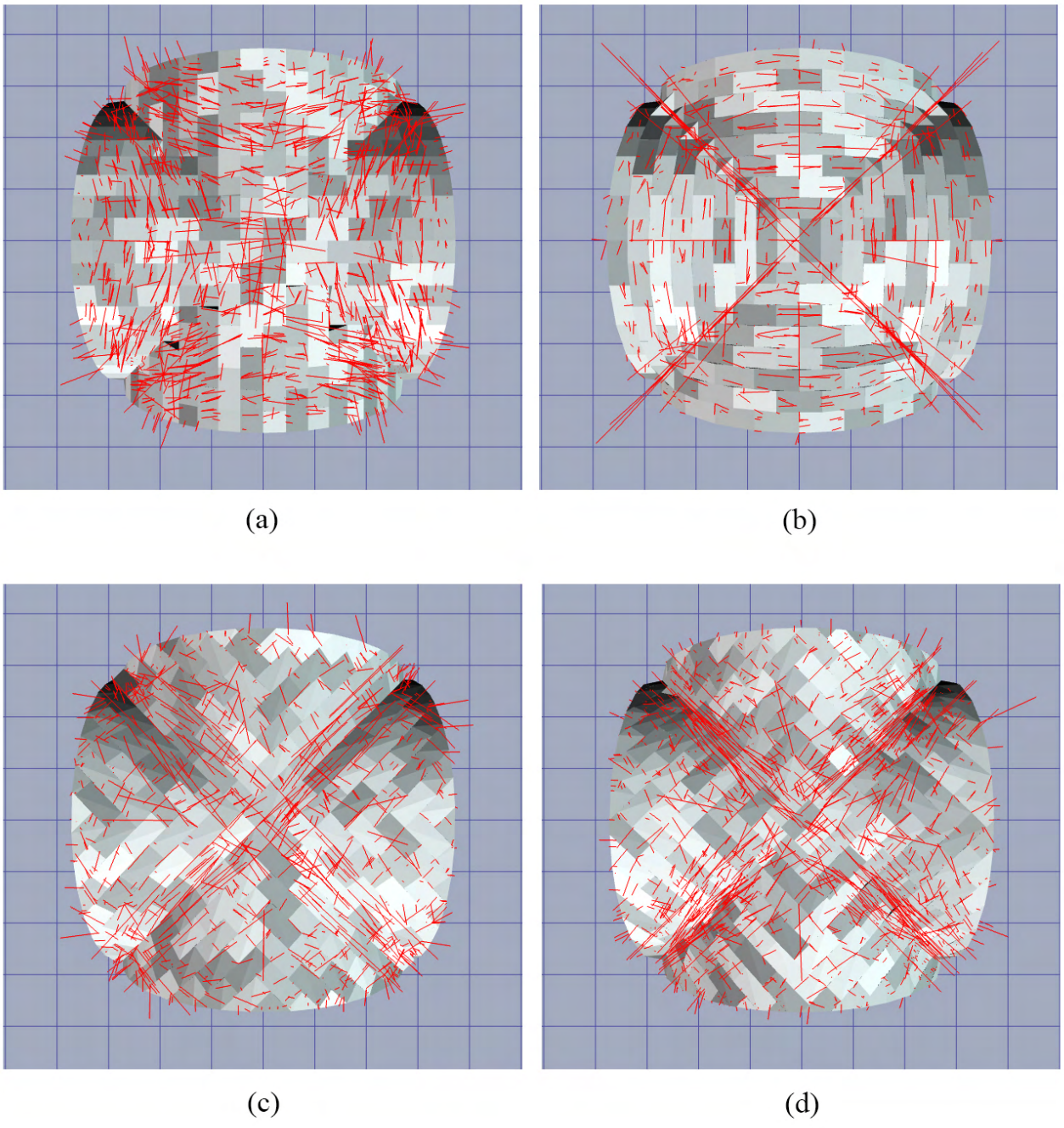

Figure 12: Forces flow in cross vaults under self-weight: (a) Brick rows perpendicular to sides; (b) Brick rows parallel to sides; (c) Brick rows parallel to diagonals; (d) Brick rows perpendicular to diagonals. Force resultant at each contact point is represented with red lines whose length is proportional to the force magnitude.

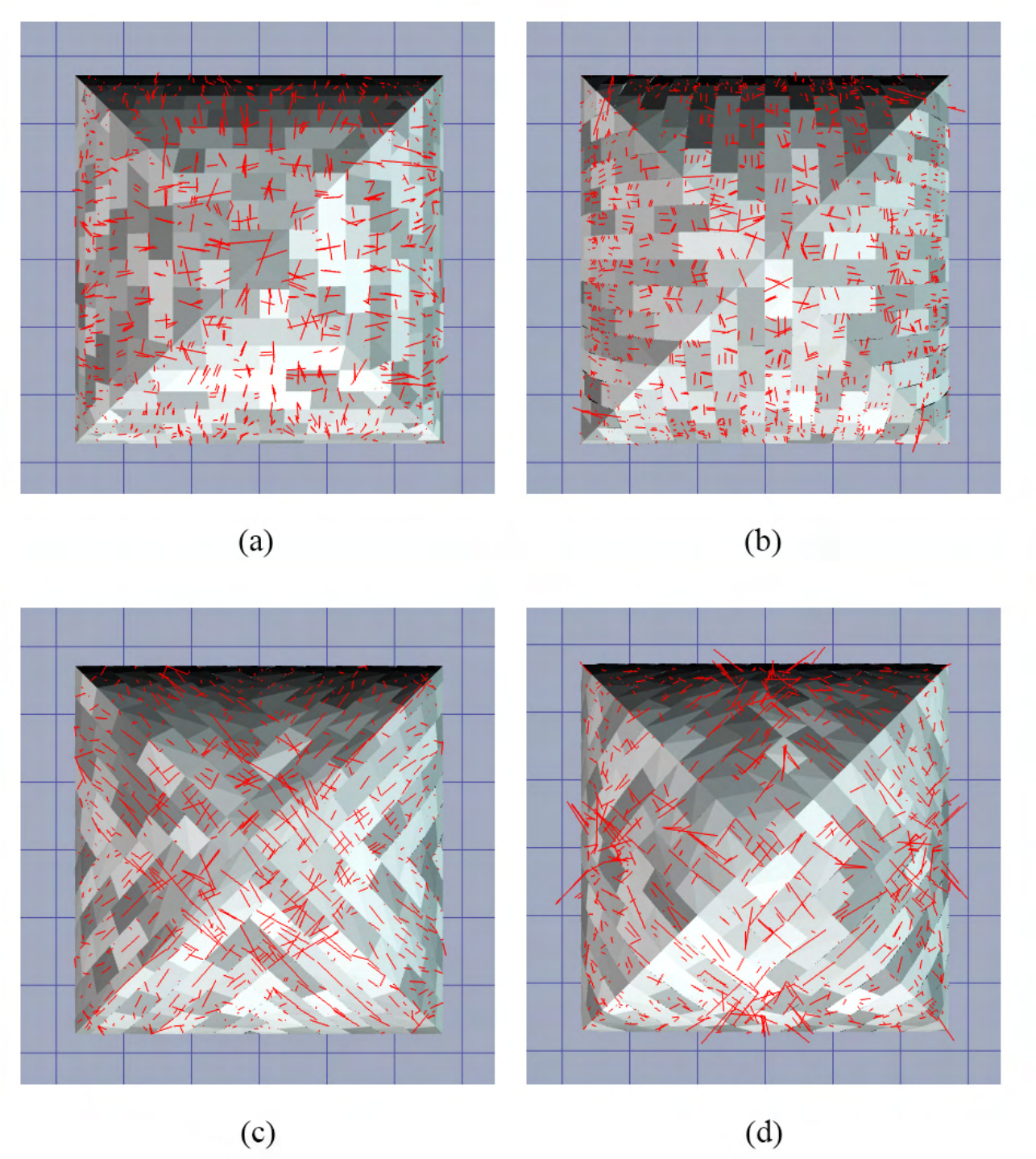

Figure 13: Forces flow in pavilion vaults under self-weight: (a) Brick rows parallel to sides; (b) Brick rows perpendicular to sides; (c) Brick rows parallel to diagonals; (d) Brick rows perpendicular to diagonals. Force resultant at each contact point is represented with red lines whose length is proportional to the force magnitude.

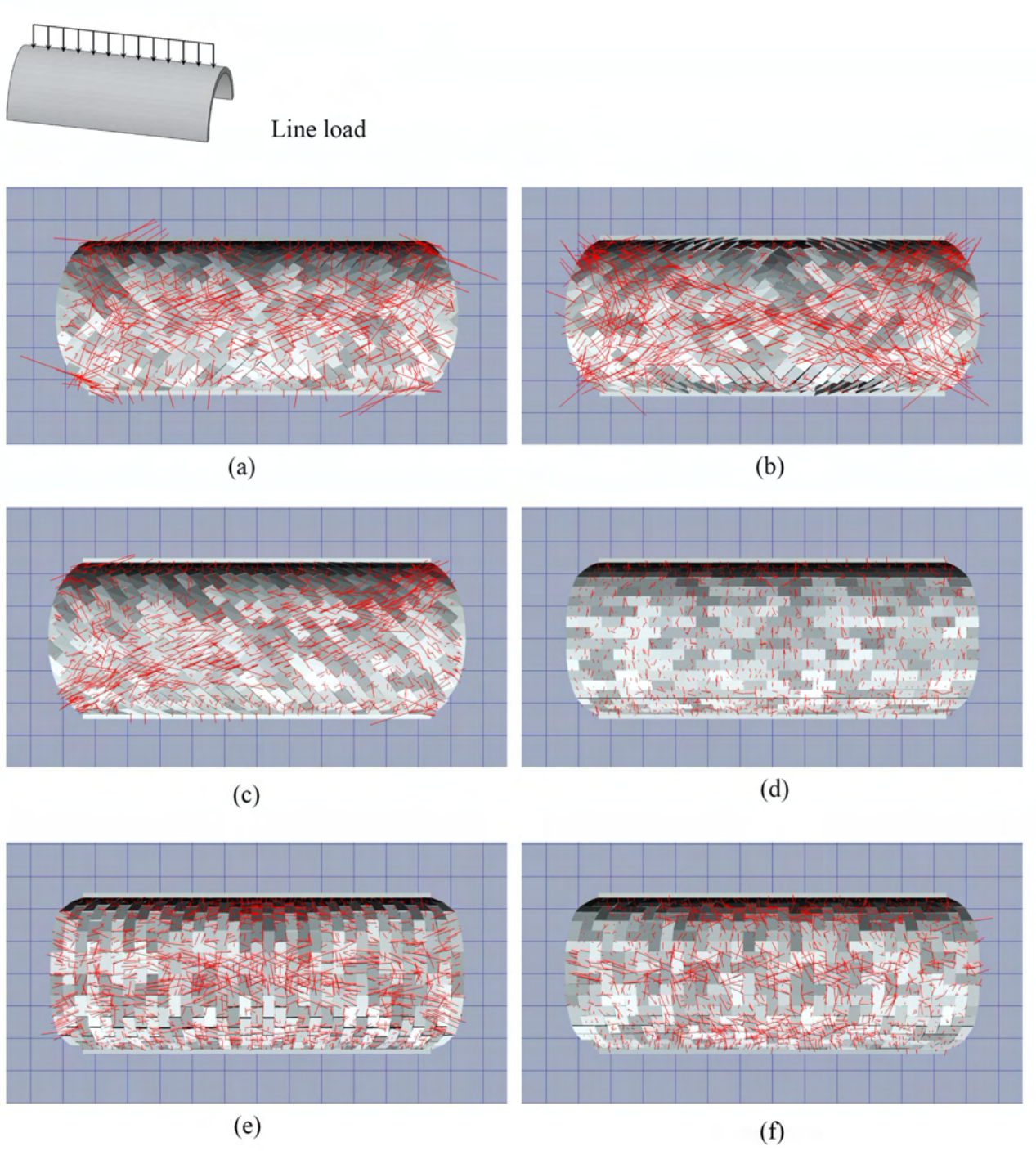

Figure 14: Forces flow in barrel vaults under line load: (a) Herringbone brick rows to the center; (b) Herringbone brick rows to edges; (c) Diagonal brick rows; (d) Brick rows parallel to supports; (e) Brick rows perpendicular to supports; (f) Bricks in a herringbone configuration. Force resultant at each contact point is represented with red lines whose length is proportional to the force magnitude.

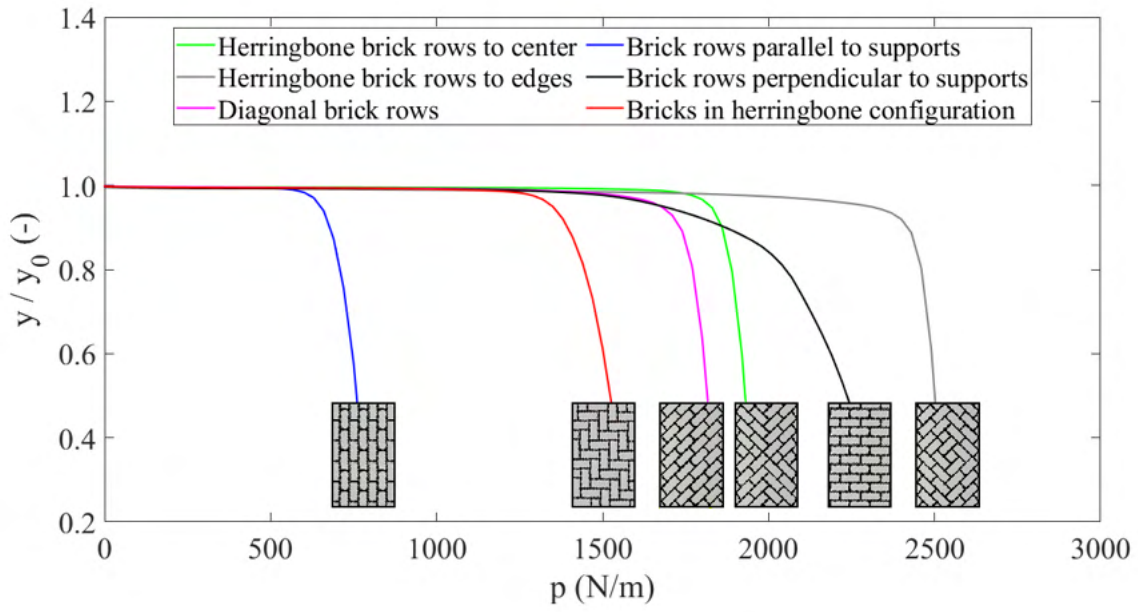

Figure 15: Barrel vaults with different brick patterns: dimensionless position of the key y/y_0 as a function of the applied load p.

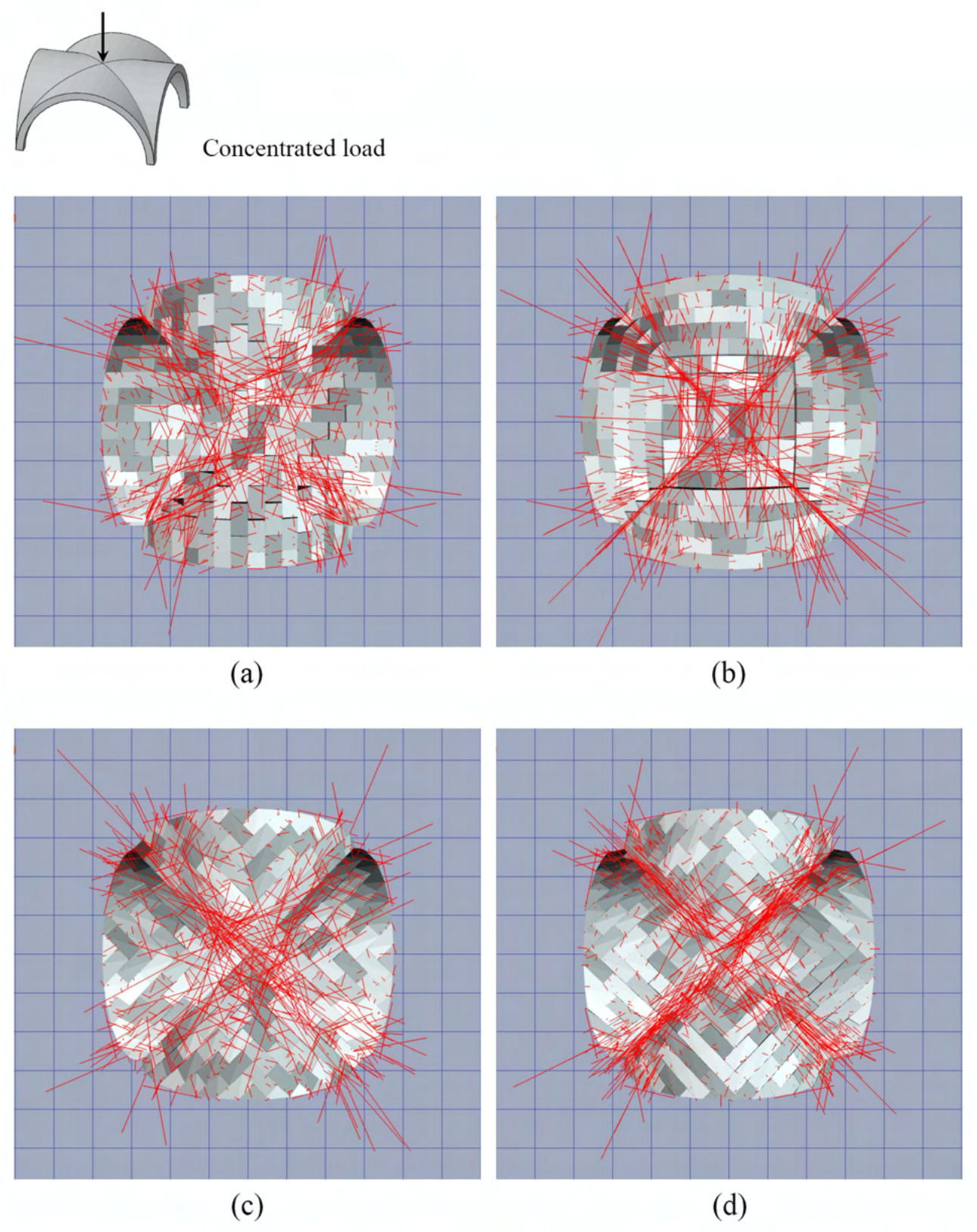

Figure 16: Forces flow in cross vaults under a concentrated force in the key: (a) Brick rows perpendicular to sides; (b) Brick rows parallel to sides; (c) Brick rows parallel to diagonals; (d) Brick rows perpendicular to diagonals. Force resultant at each contact point is represented with red lines whose length is proportional to the force magnitude.

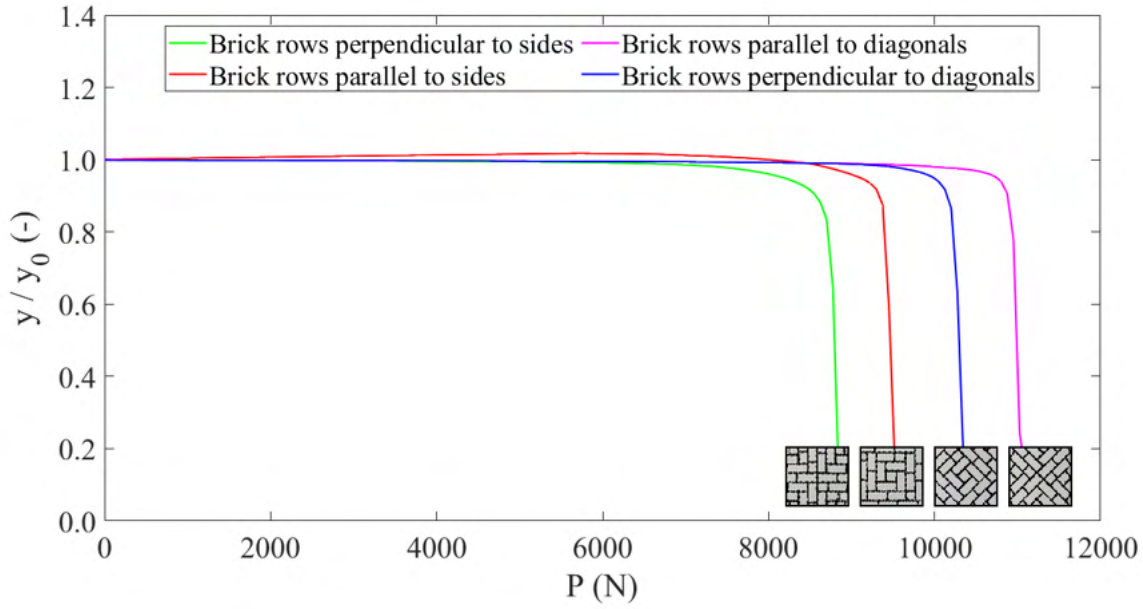

Figure 17: Cross vaults with different brick patterns: dimensionless position of the key y/y_0 as a function of the applied load P.

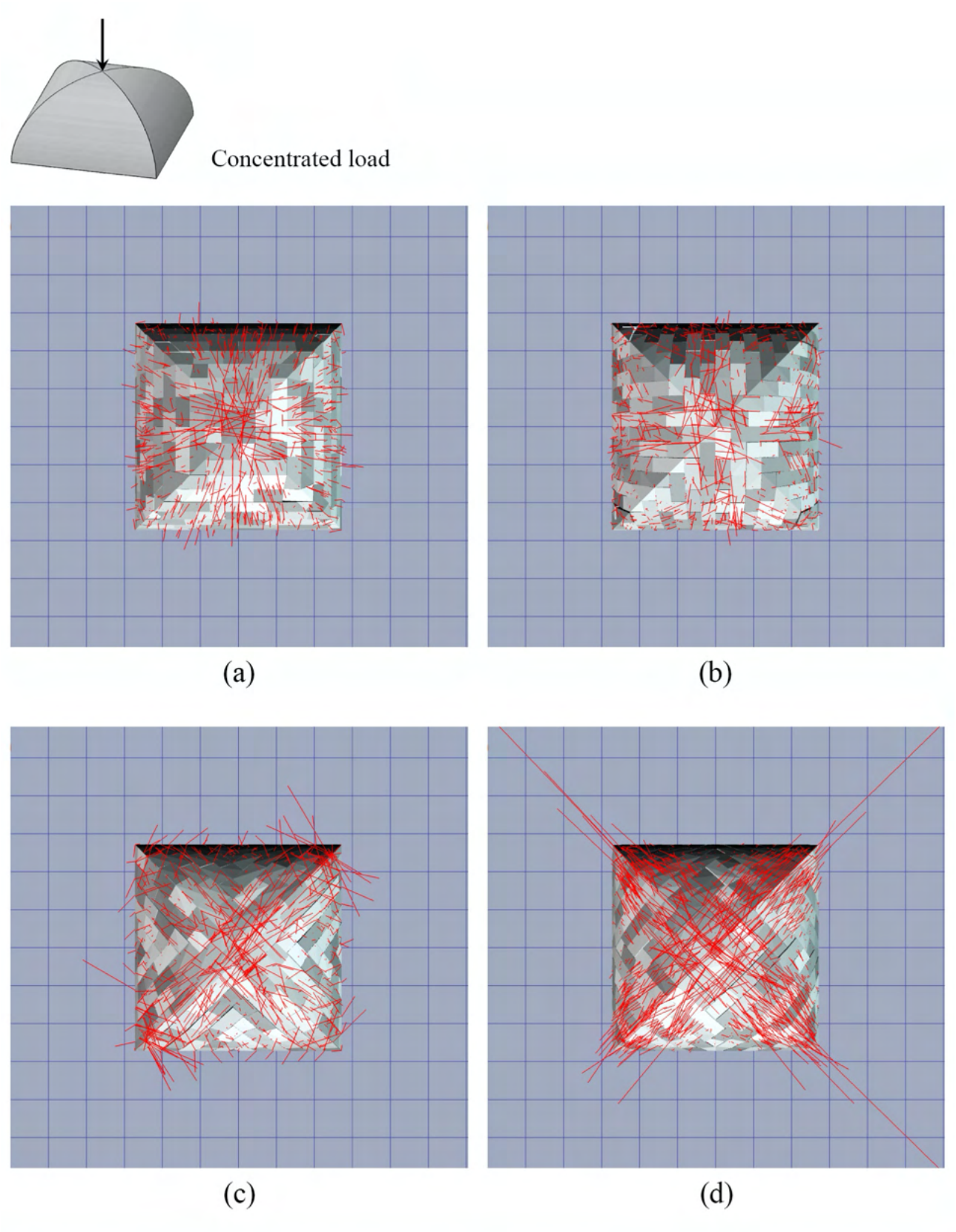

Figure 18: Forces flow in pavilion vaults under a concentrated force in the key: (a) Brick rows parallel to sides; (b) Brick rows perpendicular to sides; (c) Brick rows parallel to diagonals; (d) Brick rows perpendicular to diagonals. Force resultant at each contact point is represented with red lines whose length is proportional to the force magnitude.

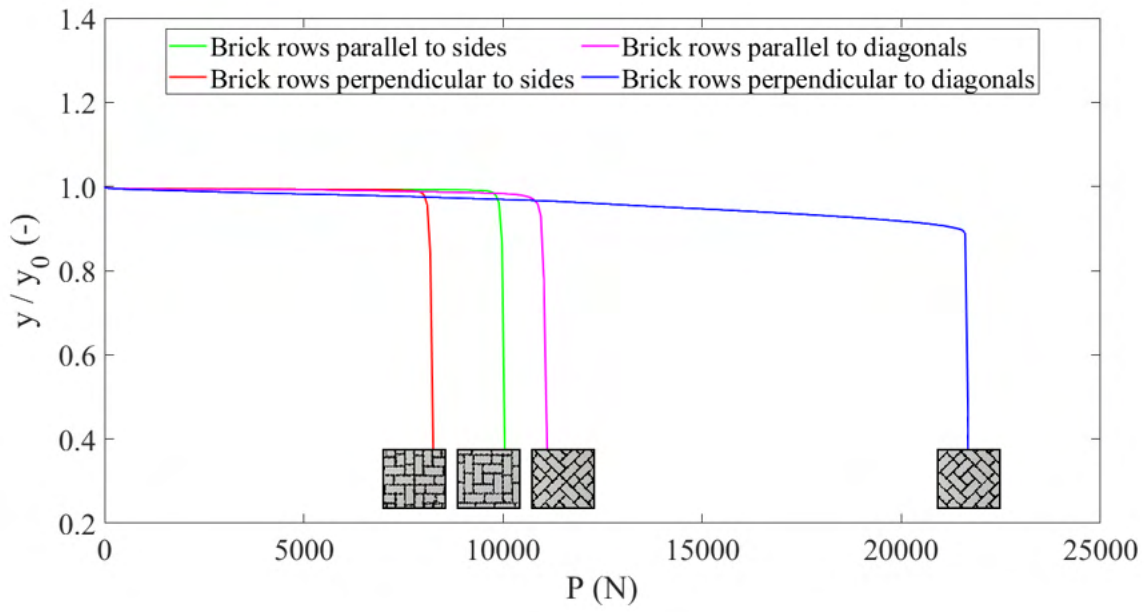

Figure 19: Pavilion vaults with different brick patterns: Dimensionless position of the key y/y_0 as a function of the applied load P.

Table 1 - Values of the parameters of the model adopted after calibration.

Parameter	**Value**
Solver	Barzilai-Borwein
Compliance	$8 \cdot 10^{-9}$ m/N
Damping	0.2 kg/s
Friction	0.5
Density	1800 kg/m^3
Envelope	$5 \cdot 10^{-3}$ m
Margin	$2 \cdot 10^{-4}$ m
Time-step	$1 \cdot 10^{-3}$ s
Time-interval	30 s
Iterations	1000